PREDICTIONS OF AXISYMMETRIC FREE TURBULENT SHEAR FLOWS
USING A GENERALIZED EDDY-VISCOSITY APPROACH*

By J. H. Morgenthaler and S. W. Zelazny
Bell Aerospace Company, Division of Textron

SUMMARY

The lack of a general theory for predicting turbulent flows has resulted in the development of various empirical techniques applicable to specific classes of these flows. One class of flows of considerable interest for many years, because of the various engineering applications, is designated as free turbulent shear flows. A generalized eddy-viscosity approach has been successfully applied to these flows and is reported. Results presented herein for the test cases selected for evaluation by the Data Selection Committee of the NASA Working Conference on Free Turbulent Shear Flows show that predictions were obtained which are adequate for most engineering applications.

Because of the importance of starting computations from the injection station where experimentally determined mean and turbulence parameters are rarely available, a very simple core model applicable to simple step-type (slug) profiles was developed. Agreement between predicted and experimental mean profiles was generally almost as good for calculations made by using this model throughout the core region and the transition model for all subsequent regions as predictions made by starting from experimental profiles in the transition region.

The generalized eddy-viscosity model, which was developed in part through correlation of turbulence parameters, successfully predicted turbulent shear stress, turbulent intensity, and mean velocity profiles for a 0.040-inch-diameter microjet. Therefore, successful scaling by the model was demonstrated since data used in its development was for jet areas up to 90 000 times as large as the microjet and velocities only 1/20th as high.

INTRODUCTION

There has been considerable interest for many years in turbulence, since most flow fields of practical importance are turbulent. Unfortunately, there is no general analytical technique available for their prediction. In fact, a group of French scientists (ref. 1) has objected to the use of a set of partial differential equations, such as

the equations of change, for application to turbulent flows; they feel that since a turbulent flow field is in "pure chaos," the instantaneous velocity of a particle of fluid cannot be sufficiently regular to satisfy the constraints of partial differential equations such as the Navier-Stokes equations. Unfortunately, no substitute for the equations of change has been proposed.

Therefore, the current approach in analysis of turbulent flows is to assume that the laminar form of the equations of change apply to instantaneous values of the velocity, density, enthalpy, and concentration. These equations are then time-averaged, such that cross correlations, that is, Reynolds transport terms, occur in addition to the original "laminar-type" terms. Evaluation of these terms requires experimental information concerning the nature of turbulence, since there are insufficient independent equations to specify a given turbulent flow uniquely. The fact that experimental data are required for specification of the Reynolds transport terms is the reason that analyses of turbulent flows, whatever the approach, must be considered semiempirical.

Two general techniques that have been used extensively to provide the needed turbulence input are the eddy-viscosity and the turbulence kinetic energy (TKE) approaches. (See refs. 2 to 4.) Both were developed primarily for the prediction of momentum transport (for example, mean velocity fields) because the velocity field was frequently of primary interest. However, as more complex applications arise such as supersonic combustors and chemical lasers, prediction of mass and energy transport becomes more important than momentum transport. At present, the assumption generally made is that turbulent Prandtl and Schmidt numbers are constant (generally less than unity, the value specified being rather arbitrary) so that the identical approach used for predicting momentum transport can be used for predicting mass and energy transport as well.

Unfortunately, the assumption of constant turbulent Prandtl and Schmidt numbers has been shown in a number of investigations to be only a rough approximation (for example, refs. 5 to 7) so that not until adequate mixing models for mass and energy transport also are devised can solution of practical problems involving multispecies turbulent flows be obtained with confidence. Of course, generality of an analysis is desirable; however, from a practical standpoint, it is not necessary (nor very likely) that all turbulent flows will be correlated with a single semiempirical mixing model. As long as flows of a given class can be predicted over the complete range of practical interest, useful computations can be made.

Several years ago, the eddy-viscosity approach was selected for further development at Bell Aerospace Company, because it appeared to have a number of advantages over the newer TKE approach (refs. 8 to 11) for application to practical combustor problems:

(1) Successful modeling techniques established for momentum transport could be applied directly to the modeling of mass and energy transport, and thereby would make the assumption of constant turbulent Schmidt, Prandtl, and Lewis numbers unnecessary.

(2) Compressible multispecie free shear layer flows were of greatest interest; such flows were not successfully treated prior to 1971 by use of the TKE approach. The simplicity and flexibility of the eddy-viscosity approach for application to practical systems such as combustors were judged to be significant.

(3) Profiles computed downstream of the injection station were less sensitive to precise initial conditions. In fact, as demonstrated, the eddy-viscosity approach permits calculations to be begun from the injector face by assuming simple (and obviously very approximate) step functions for mean velocity, mass faction, and stagnation temperature; whereas, the TKE approach requires detailed initial shear stress profiles.

(4) The eddy-viscosity approach does not require an explicit relationship between the shear stress and the TKE. At present there is a controversy as to whether the shear stress is directly proportional to the TKE or the square root of the TKE and thus its general applicability is somewhat uncertain.

(5) Empirical relationships are required for the second and higher order correlations in the TKE equation. The data used to develop these empirical relationships is limited to simple flow conditions, that is, low-speed constant-density flows. Quite possibly these relations will not apply in general to more complex practical flow systems.

(6) The TKE approach had not been demonstrated to predict successfully the details of mixing and reacting jet flow.

(7) Both the TKE and eddy-viscosity techniques use phenomenological approaches, and therefore, neither can be expected to describe the detailed physics of the flow. The success of predictions and the ease of their use are principal factors to consider in judging the relative merits of the approaches.

SYMBOLS

D	jet diameter
f	ratio of transverse to longitudinal root-mean-square values of velocity fluctuations (eq. (2))
G	radial variation function for eddy viscosity (eq. (9)); also gas
L	characteristic length (eq. (7))

M Mach number

$N_{Pr,T}$ turbulent Prandtl number

$N_{Sc,T}$ turbulent Schmidt number

R_{uv} shear correlation coefficient (eq. (1))

r radial coordinate (fig. 1)

r_1 value of r where $\dfrac{U - U_e}{U_j - U_e} = 0.99$

r_2 value of r where $\dfrac{U - U_e}{U_j - U_e} = 0.01$

T total temperature

U mean velocity in z-direction

u fluctuating velocity in text and mean axial velocity in figures

u' root-mean-square value of fluctuating axial velocity, $\sqrt{\overline{u^2}}$

v fluctuating velocity in r-direction

v' root-mean-square value of fluctuating radial velocity, $\sqrt{\overline{v^2}}$

w fluctuating tangential velocity component or $\dfrac{1 - u}{u_e}$

w' root-mean-square value of fluctuating tangential velocity, $\sqrt{\overline{w^2}}$

x,z axial coordinates

z_c velocity core length (fig. 1)

$\bar{z} = \dfrac{z}{D}$

α mass fraction

ϵ eddy viscosity

ρ mean density

τ_{ϵ} Reynolds momentum flux (shear stress)

Subscripts:

c   evaluated at center line

e   evaluated at $r = \infty$

j   evaluated at $r = 0$, $z = 0$

max   maximum value at a given z

o   evaluated at $r = o$

u   evaluated at velocity half-width

A bar over a symbol denotes a time-averaged quantity.

GENERALIZED EDDY-VISCOSITY MODEL FOR COFLOWING STREAMS

Background

When the decision was made to pursue an eddy-viscosity approach for turbulent mixing analyses, a procedure was selected which, if successful, would circumvent many of the shortcomings of previous eddy-viscosity models. Perhaps, most important was the decision to model transport of mass, momentum, and energy separately and to consider the wide range of flow conditions for the model development (refs. 5 and 12) presented in table 1. Previous investigators had demonstrated that any select set of data could be successfully correlated (refs. 13 to 19) by using various types of models and assuming the turbulent Prandtl and Schmidt numbers to be constant. Unfortunately, most of these models had rather limited application (refs. 5 and 20).

The data in table 1 include both very low-speed single-component free jets as well as supersonic compressible multispecies coflowing streams for the configuration shown in figure 1. Because of the wide range of conditions, it was apparent that some of the assumptions made by previous investigators for mathematical simplicity could not be valid. For example, the assumption that has been most frequently made for this reason

is that no variation in the transverse (radial) direction exists in either the eddy viscosity, or alternatively the eddy diffusivity of momentum. (See refs. 13 to 19.) Unfortunately, this assumption has no valid basis (ref. 12) so that a general model must be a function of radial as well as axial position.

Another important decision was to apply the computational technique for the numerical differentiation of experimental mixing data previously developed (refs. 21 to 23) prior to initiating model development. By using this procedure, designated the inverse solution technique, mean velocity and concentration profiles are differentiated once in the radial direction, each of the remaining terms in an integral form of the shear-layer equations evaluated, and the appropriate turbulent transport coefficients solved for as a function of position in the flow field. Such information was considered to be essential for successful model development. Overall mass and momentum balances were evaluated for consistency; only high quality data which yielded species mass and momentum balances to within 20 percent of their average value at each axial station were used for the modeling.

General guidelines were established for the model development which, if successfully followed, almost certainly would lead to more general eddy-viscosity-type mixing models than those previously reported:

(1) Attempt to model the structure of the turbulence, for example, shear stress and turbulent intensities, not merely mean quantities.

(2) Predictions should exhibit self-preservation in region IV (fig. 1) which are independent of jet initial conditions.

(3) Consider the lack of attainment of equilibrium of the mean and turbulence parameters upstream of the self-preservation region by using anemometry data in the model development. Failure to follow this guideline which permits consideration of flow "history" was considered an important reason for lack of generality of previous eddy-viscosity models.

(4) Use of the strong points of past models, for example, the eddy-viscosity model should yield predictions in agreement with the successful Prandtl-type model for incompressible free jet flows in the similarity region.

(5) Judge the merit of the model by comparison of predicted and experimental profiles at each axial station for which data are available. The ability to predict proper profile shapes was considered to be more important than merely obtaining agreement with experimental data along the center line.

By using these guidelines and the results obtained from the inverse solution technique, models for the maximum values of the turbulent shear stress and eddy viscosity were devised as well as their variation in the direction transverse to the flow (radial

direction). Details of this development were presented in references 5 and 12; a summary is presented herein.

Model Development

For coflowing streams, in which there is a predominant flow direction, the shear-layer equations apply; they are the same as the boundary-layer equations except for initial and boundary conditions. The classical definitions of the turbulent shear stress applicable to incompressible flows

$$\tau_\epsilon = \rho\overline{uv} = -\rho R_{uv}u'v' = \epsilon\frac{\partial U}{\partial r} \tag{1}$$

Equation (1) was used together with the assumption that the effects of density fluctuations are negligible, as is usually done in the analysis of free turbulent shear flows. This assumption has been shown to be valid for compressible flows (up to Mach 3) in which molecular weight is constant. (See ref. 24.) Empirical relations were developed for various parameters in equation (1), that is, for u', v', and R_{uv}, which permitted prediction of turbulence quantities such as τ_ϵ and u'^2, as well as mean profiles.

The data of references 25 to 30 suggested that the ratio of axial to radial turbulent intensity, as a first approximation, may be expressed only as a function of axial position, and that the ratio of radial to tangential turbulent intensity is essentially unity.

$$\frac{v'}{u'} = f^{1/2} \quad \text{and} \quad \frac{v'}{w'} \approx 1 \tag{2}$$

where

$$f = \begin{cases} 0.5 + 0.005\bar{z} & (\bar{z} \leq 100) \\ 1.0 & (\bar{z} > 100) \end{cases}$$

and

$$\bar{z} = \frac{z}{D}$$

The empirical relationship between turbulent kinetic energy and the shear stress suggested in reference 11 was used to relate the eddy viscosity to u'^2

$$\tau_\epsilon = 0.15\rho\left(u'^2 + v'^2 + w'^2\right)\frac{\partial U/\partial r}{(\partial U/\partial r)_{max}} \tag{3}$$

Therefore, by using equations (2) and (3) and assuming that the region of maximum shear occurs at the half-width of the jet r_u

$$\frac{\tau_\epsilon}{(\tau_\epsilon)_u} = \frac{\rho u'^2}{(\rho u'^2)_u} \frac{\partial U/\partial r}{(\partial U/\partial r)_u} \tag{4}$$

and

$$\frac{\epsilon}{\epsilon_u} = \frac{\rho u'^2}{(\rho u'^2)_u} \tag{5}$$

Applying equations (1), (2), and (3) at the jet half-width r_u resulted in an expression for the maximum value of the correlation coefficient

$$\left(R_{uv}\right)_u = -0.15 \frac{1 + 2f}{f^{1/2}} \tag{6}$$

The empirical relation for the maximum value of $\left(u'^2\right)_u$ that followed the general guidelines and correlated hot-wire anemometry data was (refs. 5 and 12)

$$\left(u'^2\right)_u = 0.12 \frac{\int_0^\infty |\rho U - \rho_e U_e| r \, dr}{\rho_u L} \left(\frac{\partial U}{\partial r}\right)_u \left(1 + e^{-4.6 U_j/U_e}\right) \tag{7}$$

where

$$L = r_u + \left(D - r_u\right) e^{-0.115\bar{z}}$$

Substituting equations (2), (6), and (7) into equation (1) yields an expression for the maximum value of the eddy viscosity[1]

$$\epsilon_u = \frac{0.018(1 + 2f)\left(1 + e^{-4.6 U_j/U_e}\right) \int_0^\infty |\rho U - \rho_e U_e| r \, dr}{L} \tag{8}$$

---

[1] The original model developed in reference 12 included an empirical function of density ratio. Subsequent analysis suggested that, in general, this function was not necessary and has been excluded from the model. Interestingly, Brown and Roshko (ref. 34) have shown that the mixing rate of planar shear layers also exhibits an independence of density ratio.

Variation of the eddy viscosity in the transverse (radial) direction was evaluated by using equation (5). The empirical expression $G(r/r_u)$ used to represent this radial variation was

$$\frac{\epsilon}{\epsilon_u} = \frac{\rho u'^2}{(\rho u'^2)_u} = \frac{1.05 - 0.15e^{-4.6r/r_u}}{1.0 + 0.05(r/r_u)^7} \equiv G(r/r_u) \tag{9}$$

Equations (8) and (9) define the generalized eddy-viscosity model developed for the transition region. This model, together with the assumption that $N_{Sc,T}$ and $N_{Pr,T}$ were constant, was used for predicting the mixing of the free turbulent shear flows selected by the conference data selection committee.

Discussion of Model

The eddy-viscosity model successfully followed all the general guidelines at least partially, and therefore it is unique. Several of its features deserve comment:

(1) Radial variation of ϵ and $\rho u'^2$ are included in the empirical function $\epsilon/\epsilon_u \equiv G(r/r_u)$ defined in equation (9). This function is plotted in figure 2 along with constant and variable density data of references 25 to 28 and 31 to 33 which were used for its determination. There are several reasons for the scatter of the data: (a) turbulence quantities have not become self-preserving at the axial stations for which they were available and (b) data obtained by using the inverse solution technique scatter even more than the anemometry data since numerical differentiation of experimental data is utilized in this technique. Consistency of the injected mass and momentum integral balances to better than ±10 percent (rather than ±20 percent) is required to reduce the scatter.

Nevertheless, the composite results in figure 2 strongly indicate that the eddy viscosity reaches a maximum at some distance from the center line and that it exhibits an intermittent-type behavior at the outer edge of the mixing region analogous to the behavior of boundary layers (ref. 2). The data also indicate that ϵ/ϵ_u is monotonically decreasing for $r/r_u > 1$ and that it reaches a maximum at about $r/r_u \approx 0.6$, that is, in the vicinity of half-width of the jet. The exact location of the maximum is difficult to pinpoint because of the data scatter; however, the maximum of the function defined by equation (9) occurs at $r/r_u = 0.66$. No consistent trend was apparent which correlated with density variation across the mixing region. Therefore, as a first approximation, the solid curve represented by equation (9) was used to represent the average variation of eddy viscosity in the transverse direction. This approximation is obviously superior to the assumption that ϵ/ϵ_u is constant which was frequently made by previous investigators; however, it is apparent from figure 2 that a correlation which includes other parameters than r/r_u is needed to reduce the scatter.

(2) Both the eddy viscosity and turbulent intensity u'/U_j are proportional to the mass defect. The mass defect has been successfully used by a number of investigators to model the turbulent shear stress over a wide range of flow conditions and test geometries. It was shown by Clauser (ref. 35) to correlate the eddy viscosity in the outer region of a two-dimensional turbulent incompressible boundary layer in the absence of pressure gradients. Schetz (refs. 18 and 19) extended the mass defect concept to model axisymmetric coflowing streams in the transition region. Zelazny (ref. 36) further generalized this concept to apply to both jets in a quiescent atmosphere and coflowing streams. It should also be noted that the generalized eddy-viscosity model predicts the same center-line velocity decay rate in the similarity region as the Prandtl model.

(3) Recognition was given the fact that turbulent shear stress is not determined exclusively by local mean flow properties at a particular location; that is, until the flow is in the self-preservation region (fig. 1), prior development or "history" of the flow must be considered, for example, initial conditions and wall effects. An attempt was made to include this effect in the model empirically by defining a characteristic length L (eq. (7)) and a function f (eq. (2)), both of which varied significantly with axial location in the near region up to about 100 diameters downstream ($\bar{z} = 100$).

The fact that $L = r_u$ (a function of axial position) was a more appropriate characteristic length than $L = D/2$ (a constant) was discussed in reference 36. The more sophisticated relation of equation (7) was demonstrated to yield superior predictions for the data of table 1. Figure 3 is a plot of L for several of the test cases, and shows this parameter reaches a minimum value for $\bar{z}$ ranging from 6 to 10. Since this parameter is empirical, and somewhat arbitrarily defined, its further modification may well lead to improved results.

The function f defined in equation (2) varies linearly from 0.5 at $\bar{z} = 0$ to 1.0 at $\bar{z} = 100$. It accounts empirically for the fact that u' and v' are not in equilibrium in the near region of a free shear flow. The additional refinement of considering f a function of radial position was deemed unnecessary in light of the spread of the data for u'^2 shown in figure 2.[2]

The relations L and f both attempt to allow for the fact that the free turbulent shear flows do not attain self-preserving profiles for much of the region of practical interest. (See fig. 1.) Obviously, these relations are only rough approximations for this effect since free turbulent flows do not exhibit a "universal" law by which turbulence parameters and mean properties attain self-preserving profiles. Preturbulence levels such as those caused by screens and initial profile shapes caused by splitter plates may play a significant role in determining the axial location at which this condition is achieved.

---

[2]For constant-density flows, $\dfrac{\epsilon}{\epsilon_u} = \dfrac{u'^2}{u_u'^2}$ (eq. (6)).

(4) An empirical function, $1 + \exp\left(-4.6U_j/U_e\right)$ which yields better correlation when $U_e \gg U_j$ was introduced to broaden the range of applicability. However when $U_j > U_e$, this function has a negligible effect on the eddy-viscosity model, for example, for the axisymmetric test cases the relation ranged from 1.00 to 1.04. On the other hand, a significant improvement in predictions was obtained for jets where $U_j \ll U_e$ such as those reported by Zawacki and Weinstein (ref. 25). The amplification provided by this function, which reaches a maximum value of 2, may account for the increase in the turbulent momentum transfer caused by the recirculation regions that occur in these "wake-like" flows.

Core Model

The generalized eddy-viscosity model was developed by using published data for coflowing streams. Unfortunately, there were few data available for the core region because of the difficulty in obtaining valid measurements in this region prior to the recent development of the laser-Doppler technique. Of course, a model applicable to the core is of great practical importance since in practical combustors and chemical lasers, for example, the ignition and most of the combustion occur within this region. Unfortunately, generally neither initial mean profiles nor shear stress profiles are known. The simplest type of initial condition for starting calculations would be a "step-type" or "slug" profile in which bulk mean quantities were simply used to characterize each stream. Naturally, a core mixing model appropriate to step-type initial profiles might not apply when used with experimental profiles. However, such a deficiency would not be important for modeling the transition and similarity regions as long as realistic profiles were generated prior to reaching the end of the core. An effort to develop a core model is one task of the current Bell Aerospace AFOSR contract.

As demonstrated in this paper the generalized eddy-viscosity model was quite successful in the transition region for which it was developed. The simplest possible approach was to assume a core model with the same functional form; therefore, as a first approximation, the transition model was multiplied by a constant factor (less than unity) to correct for the overmixing predicted using it in the core. The constant 0.4 proved to be satisfactory, and the "core model" which resulted, that is, $\epsilon_{core} = 0.4\epsilon_{transition}$, was far more successful than anticipated. Of course, when applying the transition model to the core region, the limits of the integral for the mass defect (eq. (8)) were changed from 0 to ∞ (the extent of the mixing zone in the transition region) to r_1 and r_2 (the extent of the mixing zone in the core). Success of this model was demonstrated by the very reasonable predictions attained when using either experimental or slug profiles at the injection station. It suggests that the general functional form of the transition model may be appropriate for the core as well; however, further work on core modeling is required before any conclusions can be drawn.

Additional efforts to model the core region are in progress at Bell Aerospace with recent results reported in reference 37. Also reported in reference 37 is a review of methods used in the modeling of turbulent axisymmetric coflowing streams and quiescent jets. Concepts such as a universal center-line mass fraction decay exponent, the Reichardt hypothesis, and a virtual origin were demonstrated generally to be inadequate for characterization of these flows.

COMPARISON OF PREDICTIONS WITH EXPERIMENTAL DATA

The generalized mixing model was used to predict the flow fields for the twelve axisymmetric jet cases and the two axisymmetric wake cases listed in table 2. The governing shear layer equations were solved numerically in the Von Mises coordinates by using an explicit finite-difference method. Three types of predictions were made: (1) Step-type (slug) initial profiles were assumed at the injection station (x = 0) and the core model used until the velocity on the center line of the jet was less than its initial (core) value; the transition model was used thereafter. (2) The first experimental profiles reported downstream of the core were used for the initial profiles (x/D designated on curve) and the transition model used exclusively. (3) The first experimental core profile was used for those cases in which the boundary-layer effects on the splitter plate were not pronounced (x/D designated on curve). (Initial velocity profiles that exhibited pronounced boundary-layer effects required a programing change to define the extent of the mixing region; this change was not deemed to be warranted in the light of the success obtained by using the slug profile.) Generally, three sets of curves are presented in each figure and correspond to each of these types of predictions. Figures are plotted in the manner specified by the data selection committee.

Test Case 6 (Maestrello and McDaid)

Predictions of the mean velocity for the high-speed quiescent jet are compared with the experimental data in figure 4 for test case 6 (ref. 38), results showed good agreement. Since no transition region profiles were available, only predictions from the injection station were possible. The predicted center-line velocities were at most 14 percent greater than the experimental velocities. This good agreement indicates that the initial slug velocity profile was adequate. However, as expected even better agreement was obtained when the actual experimental core profile (x/D = 1.0) was used. This result tends to validate the simple core model for use with realistic initial profiles.

Test Case 7 (Eggers)

Velocity data for the supersonic (Mach 2.22) quiescent jet are compared with the predictions in figure 5(a) for test case 7 (ref. 32). The agreement achieved appears to be

adequate for most engineering applications; however, the model overestimated the mixing rate (maximum error was 24 percent). Note, however, that it had underestimated the mixing rate in the previous case with a maximum error of 14 percent. Again little difference in predictions was observed when experimental core profiles were used and thus the results of the previous case were confirmed. Comparison of predicted axial velocity profiles with the data are shown in figure 5(b) for both the slug and experimental initial profiles. Good agreement was obtained at $x/r_0 = 8.0$ and adequate agreement at $x/r_0 = 27$ and 99 for each type of prediction.

Test Case 8 (Heck)

Predictions of the center-line velocity and total temperature for the high-temperature quiescent jet are shown in figures 6(a) and 6(b) for test case 8 (ref. 39). Since both momentum and thermal energy transport are significant in this case, it was necessary to specify a turbulent Prandtl number. A constant $N_{Pr,T} = 0.70$ was assumed, since this value appears to be representative of values reported in the literature. Calculations were started from the point of injection using the slug and experimental initial profiles. The former overestimated the mixing rate for both velocity and total temperature with a maximum error of 20 percent; the latter resulted in somewhat better agreement. In addition, when calculations were started from the transition region predictions of both velocity and temperature were in excellent agreement with data (maximum error was only 8 percent).

Test Case 9 (Forstall)

Predictions of the center-line velocity decay for the coflowing air (with 10 percent He tracer) mixing with airstreams are shown in figure 7(a) for test case 9 (ref. 40). The model underestimates the mixing rate with differences between prediction and experiment less than 14 percent. Examination of the initial experimental profile and the assumed initial slug profile shown in figure 7(b) suggests one reason for the disagreement. The assumed momentum flux at the injection station is considerably larger than the actual momentum flux because of significant momentum loss to the splitter plate. Therefore, mixing was predicted to be slower than actually observed. As a test of the importance of this effect, predictions also were made with a slug profile adjusted so that the momentum flux obtained from both the experimental and slug profiles would be equal (fig. 7(b)). Predicted center-line velocity decay for this case which is also presented in figure 7(a) is in excellent agreement with experimental values. In addition, calculations made by starting from the transition region show that good agreement was attained between the data and the predictions (within 10 percent).

Test Case 10 (Chriss)

Results for the high-speed, subsonic, coflowing streams of hydrogen mixing with air are shown in figure 8 for test case 10 (ref. 31). The center-line predictions obtained by using both an initial slug profile and experimental core profiles underestimated the mixing (29 percent difference for velocity and 57 percent difference for mass fraction). No significant difference was observed between these cases. Calculations started from the transition region show that slightly better agreement was obtained for the hydrogen mass fraction (within 55 percent) but poorer agreement was obtained for the center-line velocity (within 45 percent). The first experimental transition velocity profile, obtained at $x/D = 5.34$, is presented in figure 8(c). Good agreement at this station demonstrated again the adequacy of the simple core model. However, these results demonstrate that the eddy-viscosity model does not include all the complexities required for exact predictions. The predictions for this case and that of Eggers (test case 12 (ref. 41)) are the poorest of the entire set. Nevertheless, results probably still are adequate for many engineering purposes.

Test Case 11 (Eggers and Torrence)

Predictions for coflowing air (with 1 percent ethylene tracer) and airstreams are presented in figure 9 for test case 11 (ref. 7). These results show good agreement between predicted and experimental velocities and are obtained by using the initial slug profile (within 8 percent) even though data taken at the injector face exhibited boundary-layer effects at the splitter plate. Predictions also were made by starting from the transition region for this case, and they showed better agreement (within 5.5 percent).

Test Case 12 (Eggers)

Results for the Mach 0.89 inner hydrogen jet mixing with a Mach 1.32 outer airstream are presented in figure 10 for test case 12 (ref. 41). A turbulent Prandtl number of 0.9 was used in the calculations as suggested in reference 36. Predictions for velocity obtained starting both from the core and transition regions (fig. 10(a)) are somewhat low; predictions initially were 40 percent too low, but agreement was considerably better at downstream stations. The center-line hydrogen mass fraction decay (fig. 10(b)) was greatly overestimated (nearly 75 percent too low at $x/D = 6$). This overmixing is surprising, since for the similar conditions of Chriss (test case 10) the model predicted undermixing, although it gave reasonable agreement overall. Examination of the schlieren photographs of these tests suggest that pressure gradients exist in the near region (ref. 41). Of course, since the shear layer equations are used in the analysis, transverse pressure gradients could not be considered. The omission of pressure-gradient effects may, at least in part, account for the poor agreement in figure 10.

Test Case 15 (Chevray)

Predictions for an axisymmetric wake are shown in figure 11(a) for test case 15 (ref. 42). The model underestimated the mixing rate for this wake. Note, however, that the scale $w^{-3/2}$ is somewhat misleading since it amplifies small discrepancies. For example, at $x/D = 18.0$, the difference between predicted and experimental velocity is 15 percent; whereas, with respect to the $w^{-3/2}$ scale, the difference is 70 percent. Chevray also has measured the turbulent shear stress and a comparison between data and predictions is shown in figure 11(b) at $x/D = 12.0$. The predicted and experimental shear are in reasonably good agreement at this station; however, comparisons at other axial stations were not consistently this good. The ability of the model to predict turbulence quantities is discussed in the next section.

Test Case 17 (Demetriades)

Good agreement between experimental and predicted velocities was obtained for the compressible wake data presented in figure 12 for test case 17 (ref. 43). The maximum disagreement was only 8.0 percent. This result suggests that the model developed by use of jet data exclusively is reasonably valid for wake data as well.

The predictions for the wake flows were made by omitting the term $1.0 + \exp\left(-4.6U_j/U_e\right)$, from the model since actual wake data were not used in the development of this expression $\left(\text{for which } U_j = 0\right)$. Calculations made by including this term improved agreement with the Chevray data but agreement between predictions and the Demetriades data became poorer. Additional wake data must be evaluated before an empirical velocity ratio expression can be validated.

Optional Test Cases

Predictions also were made for the five optional test cases (figs. 13 to 17) which utilized axisymmetric geometry. Since the previous cases showed that valid results were obtained by starting with the initial slug profile, and since such profiles are the simplest to use, predictions were made only with these profiles.

The agreement obtained between the predictions and the experimental data for test case 18 (Wygnanski and Fiedler, refs. 29 and 30) was outstanding; that is, similar (region III, fig. 1) velocity profiles were predicted. Agreement for test case 19 (Heck, ref. 39) was also quite good (within 20 percent) as it had been for the earlier test case 8 (Heck, ref. 38). The velocity agreement is not very good (within 33 percent) for test case 20 (Chriss, ref. 44); however, the hydrogen concentration for this case was somewhat better (about 29 percent). As before, agreement was not good for either velocity or concentration for test case 21 (Chriss, ref. 31) (nearly 16 percent for velocity and 100 percent for concentration). Agreement for test case 22 (Eggers, ref. 41) also was not good; the

model drastically overestimated the mixing rate as it had for test case 12 (Eggers, ref. 41). Lack of agreement is not surprising since the data exhibits an anomalous behavior in which the center-line jet velocity becomes less than the free-stream velocity, evidence that severe pressure gradients may have occurred. For this reason, an analysis using shear-layer equations may not be appropriate.

PREDICTION OF TURBULENCE PARAMETERS

In the development of the generalized eddy-viscosity model, an effort was made to correlate both turbulence and mean quantities. Recently purchased hot wire and laser-Doppler anemometers are being used to characterize the flow from small jets in an effort to obtain empirical correlations for jet noise. Such data present an excellent opportunity to compare turbulence parameters predicted by using the model directly with experimental parameters. If successful in these predictions, the model might be used with some confidence in the development of an empirical correlation for noise.

Results of hot-wire measurements made for a 1.02-mm-diameter (0.040-in.) free jet by Baker, Moon et al. (ref. 45) are presented in figures 18 to 21; initial jet velocity was 213.4 m/sec (700 ft/sec). The data are very consistent since variation in momentum balances was less than 2.5 percent from the mean value, that is, $\int_0^\infty \rho U^2 r \, dr$ ranged from 0.0512 to 0.0533 N (0.01152 to 0.01198 lbf). Predictions were made by using the initial slug profile and the core model in the near region followed by the transition model as previously described. Agreement is seen to be very adequate for turbulent shear stress τ_ϵ, axial turbulent intensity u'/U_j, and mean velocity U_j. In the case of τ_ϵ and u'/U_j, agreement was poorest at the initial station (x = 30.48 mm (1.2 in.)) where the x-wire is long (1.27 mm (0.050 in.)) relative to the jet diameter. For this reason, characterization of the near region, that is, core and transition, are in progress using the laser-Doppler technique. The agreement between experimental and predicted velocities using the model (fig. 20) is outstanding, even at the initial station. The accuracy of predictions of mean values (within 2 percent) is significantly better than the shear stress (within 20 percent). This result demonstrates that predicted mean values exhibit a degree of insensitivity to the inaccuracies introduced in predicting the shear stress. That is, the eddy viscosity is used directly for computation of shear stress, but it merely influences a coefficient used in the numerical integration procedure to obtain mean velocity. The center-line velocity is plotted as a function of axial position in figure 21. The decay exponent is correctly given by -1 for both experimental and predicted results as is appropriate for flow in the similarity region.

Additional experiments were made for a sonic free jet; although exact static pressure matching was not attained at the nozzle exit agreement between predicted and experimental parameters, it was essentially as good as that shown in figures 18 to 20.

These results enhance our confidence in the applicability of the model for engineering calculations. They also showed the model was useful for scaling since data used for its development (table 1) were for jet areas up to 90 000 times as large as the 1.02-mm (0.040-in.) microjet and velocities 1/20th as high. No modification of the model was made for the microjet predictions.

CONCLUSIONS AND RECOMMENDATIONS

Generalized eddy-viscosity models developed for the similarity, transition, and core regions were presented which did creditable jobs of predicting mean velocity profiles (and reasonably well for concentration and temperature profiles when appropriate) for most of the 14 axisymmetric free turbulent shear flows selected by the data selection committee. The core model was demonstrated to be reasonably valid even when slug (step-type) profiles were assumed at the injector. Results established the validity of the eddy-viscosity approach for engineering predictions including practical hardware design and its optimization. (For example, see ref. 46.)

The model also was shown to predict turbulence shear stress and axial turbulence intensity as well as mean velocity for jets varying in area by a factor of 90 000 and velocities varying twentyfold. Its applicability over a wide range of jet geometries as well as flow conditions was thereby established.

The model has several important features; it includes (1) a transverse (radial) variation of the eddy viscosity, (2) the mass defect, (3) allowance for the fact that turbulent shear is not dependent exclusively on local mean flow properties (by defining an empirical characteristic length, and a function allowing for axial variation in the ratio of the axial to radial turbulence intensities), and (4) allowance for the variation in the ratio of jet velocity to external stream velocity.

The assumption of constant turbulent Schmidt and Prandtl numbers was made in order to predict flow fields in which mass and energy transport occurred in addition to momentum transport. In order to obtain satisfactory predictions, these parameters were varied from 0.6 to 0.9. These results clearly demonstrate the need for separate models for mass and energy if realistic predictions are to be made without the benefit of prior experimental data.

The critical guideline used in the development of the generalized eddy-viscosity model was application of the inverse solution technique to a wide range of valid experimental data so that quantitative results were available for determination of the various func-

tional relations and constants. The same technique should be applied for the development of turbulent mixing models for mass and energy transport, so that the unacceptable assumption that the turbulent Schmidt and Prandtl numbers are constant can be relaxed.

Examination of those workshop cases in which poorest predictions were obtained indicates that the ratio $(\rho U)_j / (\rho U_e)_e \leqq 0.6$. This result suggests that further improvement of the eddy-viscosity model may be possible by including an appropriate relation containing this ratio.

Examination of available free turbulent shear flow data suggests that more detailed experimental investigations be conducted. These investigations should include the following effects: (1) pressure gradients and pressure levels other than atmospheric, (2) initial conditions at the injection station, (3) heavy gas jets exhausting into light gases, for example, oxygen into hydrogen, and (4) jet to free-stream velocity ratios near unity.

REFERENCES

1. Pai, Shih-I: Viscous Flow Theory. II – Turbulent Flow. D. Van Nostrand Co., Inc., c.1957.

2. Hinze, J. O.: Turbulence. McGraw-Hill Book Co., Inc., 1959.

3. Kline, S. J.; Morkovin, M. V.; Sovran, G.; and Cockrell, D. J., eds.: Computation of Turbulent Boundary Layers – 1968 AFOSR-IFP-Stanford Conference. Vol. I – Methods, Predictions, Evaluation and Flow Structure. Stanford Univ., c.1969.

4. Nash, John F.; and Patel, Virendra C.: Three-Dimensional Turbulent Boundary Layers. SBC Technical Books, 1972.

5. Zelazny, S. W.; Morgenthaler, J. H.; and Herendeen, D. L.: Reynolds Momentum and Mass Transport in Axisymmetric Coflowing Streams. Proceedings of the 1970 Heat Transfer and Fluid Mechanics Institute, Turbot Sarpkaya, ed., c.1970, pp. 135-152.

6. Peters, C. E.; Chriss, D. E.; and Paulk, R. A.: Turbulent Transport Properties in Subsonic Coaxial Free Mixing Systems. AIAA Paper 69-681, June 1969.

7. Eggers, James M.; and Torrence, Marvin G.: An Experimental Investigation of the Mixing of Compressible-Air Jets in a Coaxial Configuration. NASA TN D-5315, 1969.

8. Glushko, G. S.: Turbulent Boundary Layer on a Flat Plate in an Incompressible Fluid. Bull. Acad. Sci. USSR, Mech. Ser., no. 4, 1965, pp. 13-23. (Available in English translation from DDC as AD 638 204, May 1966.)

9. Patankar, S. V.; and Spalding, D. B.: A Finite-Difference Procedure for Solving the Equations of the Two-Dimensional Boundary Layer. Int. J. Heat & Mass Transfer, vol. 10, no. 10, Oct. 1967, pp. 1389-1411.

10. Bradshaw, P.; Ferriss, D. H.; and Atwell, N. P.: Calculation of Boundary-Layer Development Using the Turbulent Energy Equation. J. Fluid Mech., vol. 28, pt. 3, May 26, 1967, pp. 593-616.

11. Lee, S. C.; and Harsha, P. T.: Use of Turbulent Kinetic Energy in Free Mixing Studies. AIAA J., vol. 8, no. 6, June 1970, pp. 1026-1032.

12. Zelazny, S. W.; Morgenthaler, J. H.; and Herendeen, D. L.: Shear Stress and Turbulent Intensity Models for Coflowing Axisymmetric Streams. AIAA Paper 72-47, Jan. 1972.

13. Zakkay, Victor; Krause, Egon; and Woo, Stephen D. L.: Turbulent Transport Properties for Axisymmetric Heterogeneous Mixing. PIBAL Rep. No. 813 (Contract AF 33(616)-7661), Polytech. Inst. Brooklyn, Mar. 1964. (Available from DDC as AD 460 970.)

14. Ferri, Antonio; Libby, Paul A.; and Zakkay, Victor: Theoretical and Experimental Investigation of Supersonic Combustion. ARL 62-467, U.S. Air Force, Sept. 1962.

15. Ferri, Antonio; Libby, Paul A.; and Zakkay, Victor: Theoretical and Experimental Investigation of Supersonic Combustion. PIBAL-713 (Contract AF 49(638)-217), Polytech. Inst. Brooklyn, Sept. 1962.

16. Donaldson, Coleman duP.; and Gray, K. Evan: Theoretical and Experimental Investigation of the Compressible Free Mixing of Two Dissimilar Gases. AIAA J., vol. 4, no. 11, Nov. 1966, pp. 2017-2025.

17. Cohen, L. S.: A New Kinematic Eddy Viscosity Model. Rep. G211709-1, United Aircraft Corp., Jan. 1968.

18. Schetz, Joseph A.: Turbulent Mixing of a Jet in a Coflowing Stream. AIAA J., vol. 6, no. 10, Oct. 1968, pp. 2008-2010.

19. Schetz, Joseph A.: Unified Analysis of Turbulent Jet Mixing. NASA CR-1382, 1969.

20. Harsha, Philip Thomas: Free Turbulent Mixing: A Critical Evaluation of Theory and Experiment. AEDC-TR-71-36, U.S. Air Force, Feb. 1971. (Available from DDC as AD 718 956.)

21. Morgenthaler, John H.: Supersonic Mixing of Hydrogen and Air. NASA CR-747, 1967.

22. Morgenthaler, John H.; and Marchello, Joseph M.: Turbulent Transport Coefficients in Supersonic Flow. Int. J. Heat & Mass Transfer, vol. 9, no. 12, Dec. 1966, pp. 1401-1418.

23. Morgenthaler, J. H.: Mixing in High Speed Flow. Rep. No. 9500-920143, Bell Aerosystems Co., Oct. 1968.

24. Bradshaw, P.; and Ferriss, D. H.: Calculation of Boundary-Layer Development Using the Turbulent Energy Equation. II — Compressible Flow on Adiabatic Walls. NPL Aero Rep. 1217, Brit. A.R.C., Nov. 24, 1966.

25. Zawacki, Thomas S.; and Weinstein, Herbert: Experimental Investigation of Turbulence in the Mixing Region Between Coaxial Streams. NASA CR-959, 1968.

26. Sami, Sedat: Velocity and Pressure Fields of a Diffusing Jet. Ph. D. Diss., Univ. of Iowa, 1966.

27. Sami, Sedat: Balance of Turbulence Energy in the Region of Jet-Flow Establishment. J. Fluid Mech., vol. 29, pt. 1, July 18, 1967, pp. 81-92.

28. Sami, Sedat; Carmody, Thomas; and Rouse, Hunter: Jet Diffusion in the Region of Flow Establishment. J. Fluid Mech., vol. 27, pt. 2, Feb. 2, 1967, pp. 231-252.

29. Wygnanski, I.; and Fiedler, H.: Some Measurements in the Self Preserving Jet. D1-82-0712, Flight Sci. Lab., Boeing Sci. Res. Lab., Apr. 1968.

30. Wygnanski, I.; and Fiedler, H.: Some Measurements in the Self-Preserving Jet. J. Fluid Mech., vol. 38, pt. 3, Sept. 18, 1969, pp. 577-612.

31. Chriss, D. E.: Experimental Study of the Turbulent Mixing of Subsonic Axisymmetric Gas Streams. AEDC-TR-68-133, U.S. Air Force, Aug. 1968. (Available from DDC as AD 672 975.)

32. Eggers, James M.: Velocity Profiles and Eddy Viscosity Distributions Downstream of a Mach 2.22 Nozzle Exhausting to Quiescent Air. NASA TN D-3601, 1966.

33. Gibson, M. M.: Spectra of Turbulence in a Round Jet. J. Fluid Mech., vol. 15, pt. 2, Feb. 1963, pp. 161-173.

34. Brown, Garry; and Roshko, Anatol: The Effect of Density Difference on the Turbulent Mixing Layer. Turbulent Shear Flows, AGARD-CP-93, Jan. 1972, pp. 23-1 — 23-12.

35. Clauser, Francis H.: The Turbulent Boundary Layer. Vol. IV of Advances in Applied Mechanics, H. L. Dryden and Th. von Kármán, eds., Academic Press, Inc., 1956, pp. 1-51.

36. Zelazny, Stephen W.: Eddy Viscosity in Quiescent and Coflowing Axisymmetric Jets. AIAA J., vol. 9, no. 11, Nov. 1971, pp. 2292-2294.

37. Zelazny, Stephen William: Modeling of Turbulent Axisymmetric Coflowing Streams and Quiescent Jets: A Review and Extension. Ph. D. Diss., State Univ. of New York at Buffalo, Sept. 1972.

38. Maestrello, L.; and McDaid, E.: Acoustic Characteristics of a High-Subsonic Jet. AIAA J., vol. 9, no. 6, June 1971, pp. 1058-1066.

39. Heck, P. H.: Jet Plume Characteristics of 72-Tube and 72-Hole Primary Suppressor Nozzles. T.M. No. 69-457 (FAA Contract FA-SS-67-7), Flight Propulsion Div., Gen. Elec. Co., July 1969.

40. Forstall, Walton, Jr.; and Shapiro, Ascher H.: Momentum and Mass Transfer in Coaxial Gas Jets. J. Appl. Mech., vol. 17, no. 4, Dec. 1950, pp. 399-408.

41. Eggers, James M.: Turbulent Mixing of Coaxial Compressible Hydrogen-Air Jets. NASA TN D-6487, 1971.

42. Chevray, R.: The Turbulent Wake of a Body of Revolution. Trans. ASME, Ser. D: J. Basic Eng., vol. 90, no. 2, June 1968, pp. 275-284.

43. Demetriades, Anthony: Mean-Flow Measurements in an Axisymmetric Compressible Turbulent Wake. AIAA J., vol. 6, no. 3, Mar. 1968, pp. 432-439.

44. Chriss, D. E.; and Paulk, R. A.: An Experimental Investigation of Subsonic Coaxial Free Turbulent Mixing. AEDC-TR-71-236 (AFOSR-72-0237TR), U.S. Air Force, Feb. 1972. (Available from DDC as AD 737 098.)

45. Baker, A. J.; Moon, L. F.; Morgenthaler, J. H.; and Peschke, W. T.: Project 8(R) Fluid Mechanics and Combustion Technology. Rep. No. 9500-920246, Bell Aerospace Co., Jan. 1972.

46. Morgenthaler, J. H.; Zelazny, S. W.; and Herendeen, D. L.: Combustor Correlation Technique. AIAA Paper No. 72-1074, Nov.-Dec. 1972.

47. Alpinieri, Louis J.: Turbulent Mixing of Coaxial Jets. AIAA J., vol. 2, no. 9, Sept. 1964, pp. 1560-1567.

TABLE 1.- COAXIAL JET MIXING DATA USED IN MODEL DEVELOPMENT

[External gas stream was air in all cases]

Investigator	Case number	Jet gas	D, mm	D, in.	ρ_j, kg/m³	ρ_j, lbm/ft³	U_j, m/sec	U_j, ft/sec	$(z/D_j)_{min}$	$(z/D_j)_{max}$	$\dfrac{(U)_j}{(U)_e}$	$\dfrac{(\rho u)_j}{(\rho u)_e}$	$\dfrac{(\rho u^2)_j}{(\rho u^2)_e}$	M_j	M_e
Chriss (ref. 31)	*1	H_2	12.7	0.5	87.6	5.47×10^{-3}	1005.8	3300	2.95	14.55	6.300	0.560	3.520	0.79	0.42
	*2	H_2	12.7	.5	92.7	5.79	975.4	3200	.49	14.50	4.400	.390	1.710	.79	.60
	*3	H_2	12.7	.5	87.8	5.48	929.6	3050	.42	20.80	3.800	.320	1.210	.73	.66
	*4	H_2	12.7	.5	85.7	5.35	731.5	2400	.50	20.80	3.000	.240	.720	.57	.67
	*5	H_2	12.7	.5	82.7	5.16	579.1	1900	.41	12.70	2.400	.190	.460	.44	.65
	6	H_2	12.7	.5	80.7	5.04	944.9	3100	.50	19.20	4.600	.620	2.850	.71	.42
	7	H_2	12.7	.5	79.3	4.95	746.8	2450	.50	16.30	3.200	.410	1.310	.56	.49
	8	H_2	12.7	.5	74.0	4.62	594.4	1950	.51	12.40	2.500	.300	.750	.43	.50
	9	Air	12.7	.5	1322.4	82.56	286.5	940	.50	14.30	2.400	3.600	8.650	.87	.71
Zakkay (ref. 13)	*1	H_2	7.6	.3	48.2	3.01	603.5	1980	10.0	30.00	1.460	.047	.069	.51	1.6
	2	H_2	7.6	.3	64.1	4.00	701.0	2300	13.3	30.00	1.690	.072	.122	.60	1.6
	3	H_2	7.6	.3	76.9	4.80	1002.8	3290	13.3	30.00	2.420	.124	.300	.89	1.6
	*4	He	7.6	.3	141.0	8.80	454.2	1490	13.3	30.00	1.100	.103	.113	.51	1.6
	5	He	7.6	.3	163.4	10.2	691.9	2270	13.3	26.70	1.670	.185	.309	.82	1.6
	6	Ar	7.6	.3	1633.8	102.0	219.5	720	13.3	30.00	.530	.590	.312	.82	1.6
	7	Ar	7.6	.3	2066.3	129.0	231.6	760	13.3	26.70	.560	.790	.442	.89	1.6
	8	Ar	7.6	.3	2354.6	147.0	256.0	840	16.7	30.00	.620	.976	.605	1.00	1.6
Eggers (ref. 32)	*1	Air	25.4	1.0	2402.7	150.0	539.2	1769	.0	75.00				2.22	.0
Eggers and Torrence (ref. 7)	*1	Air/ethylene	24.4	.96	1457.6	91.0	289.6	950	.0	49.00	.740	.640	.447	.90	1.3
Alpinieri (ref. 47)	1	CO_2	50.8	2.0	2162.4	135.0	95.1	312	5.25	12.50	.470	.660	.310		
	*2	CO_2	50.8	2.0	2226.5	139.0	128.6	422	5.25	12.50	.650	.950	.617		
	3	CO_2	50.8	2.0	2114.4	132.0	154.2	506	5.25	12.50	.780	1.170	.912		
Zawacki and Weinstein (ref. 25)	*1	Air	18.14	.714	1217.4	76.0	.366	1.20	.0	11.30	.025	.025	.001		
	*2	Air	18.14	.714	1217.4	76.0	.503	1.65	.0	11.30	.035	.036	.001		
	3	Air	18.14	.714	1217.4	76.0	.920	3.02	.0	14.00	.063	.063	.004		
	*4	Air	18.14	.714	1217.4	76.0	1.829	6.00	.0	14.00	.125	.125	.063		
	*5	Air	18.14	.714	1217.4	76.0	4.328	14.2	.0	21.00	.294	.294	.089		
	6	Air	18.14	.714	1217.4	76.0	14.630	48.0	1.40	14.00	1.000	1.000	1.000		
	7	Freon 12	18.14	.714	4869.5	304.0	1.207	3.96	.35	14.00	.086	.344	.030		
	*8	Freon 12	18.14	.714	4837.4	302.0	2.621	8.60	.35	21.60	.179	.714	.127		
	*9	Freon 12	18.14	.714	4869.5	304.0	1.341	4.4	.35	14.00	.185	.740	.137		
	*10	Freon 12	18.14	.714	4837.4	302.0	.564	1.85	.35	14.00	.132	.526	.070		
Sami (refs. 26 to 28)	*1	Air	304.8	12.0	1217.4	76.0	10.668	35.0	1.00	10.00					
Wygnanski (refs. 29 and 30)	†1	Air	25.5	1.004	1217.4	76.0	57.912	190.0	5.00	100.00					

*(1) Momentum integral balances were within 4 percent of their average value at any axial station.
  (2) Injected mass integral balances were within 20 percent of their average value at any axial station and were within 13 percent of their average value at 80 percent of the axial stations.
  †Detailed profiles not available.

TABLE 2.- AXISYMMETRIC FREE TURBULENT SHEAR LAYER DATA FOR NASA LANGLEY WORKSHOP TEST CASES

Investigator	Test case	Jet gas	D, mm	D, in.	ρ_j, kg/m³	ρ_j, lbm/ft³	U_j, m/sec	U_j, ft/sec	U_e, m/sec	U_e, ft/sec	$(z/D_j)_{min}$	$(z/D_j)_{max}$	$\dfrac{(U)_j}{(U)_e}$	$\dfrac{(\rho U)_j}{(\rho U)_e}$	$\dfrac{(\rho U^2)_j}{(\rho U^2)_e}$	M_j	M_e
Maestrello and McDaid (ref. 38)	6	Air	61.98	2.44	1.310	0.0818	211.2	693.0	0	0.0	1.0	39.6	∞	∞	∞	0.65	0.0
Eggers (ref. 32)	7	Air	25.578	1.007	2.404	.1501	539.19	1769.0	0	.0	.0	74.7	∞	∞	∞	2.22	.0
Heck (ref. 39)	8	Air	109.22	4.30	.532	.0332	318.52	1045.0	0	.0	2.79	19.53	∞	∞	∞	.70	.0
Forstall (ref. 40)	9	[a]Air	6.35	.25	1.113	.0695	36.58	120.0	9.144	30.0	.0	80.0	4.0	3.7	14.8	.10	.03
Chriss (ref. 31)	10	H_2	12.7	.50	.088	.0055	1005.84	3300.0	157.58	517.0	2.97	14.55	6.3	.56	3.52	.79	.421
Eggers and Torrence (ref. 7)	11	[b]Air	24.384	.96	1.458	.091	289.56	950.0	390.14	1280.0	.0	49.0	.74	.64	.47	.9	1.3
Eggers (ref. 41)	12	H_2	11.608	.457	.096	.00601	1074.12	3524.0	394.11	1293.0	.0	63.0	2.72	.163	.443	.89	1.32
Chevray (ref. 42)	15	Air	254.00	[c]10.0	1.217	.0760	------	------	27.43	90.0	.0	18.0	----	----	----	----	.09
Demetriades (ref. 43)	17	Air	3.962	[d].156	----	------	------	------	679.09	2228.0	17.0	58.7	----	----	----	----	2.94
Wygnanski and Fiedler (refs. 29 and 30)	18	Air	26.416	1.04	1.217	.0760	58.52	192.0	0	.0	5.0	100.0	----	----	----	.18	.0
Heck (ref. 39)	19	Air	109.22	4.3	.392	.0245	841.86	2762.0	0	.0	2.79	19.53	----	----	----	1.41	.0
Chriss and Paulk (ref. 44)	20	[e]Air	12.7	.5	.625	.0390	121.92	400.0	58.52	192.0	1.92	18.10	2.08	1.98	4.13	.26	.13
Chriss (ref. 31)	21	H_2	12.7	.5	.086	.0054	746.76	2450.0	233.48	766.0	2.58	16.32	3.20	.44	1.40	.55	.49
Eggers (ref. 41)	22	H_2	11.608	.457	.096	.0060	1109.47	3640.0	606.55	1990.0	.0	58.0	1.83	.06	.11	.91	2.50

[a] 10 percent helium tracer by volume.
[b] 1 percent ethylene tracer by volume.
[c] Six to one prolate spheroid, 5 ft long.
[d] Base diameter of a suspended rod.
[e] 2 percent hydrogen tracer by volume.
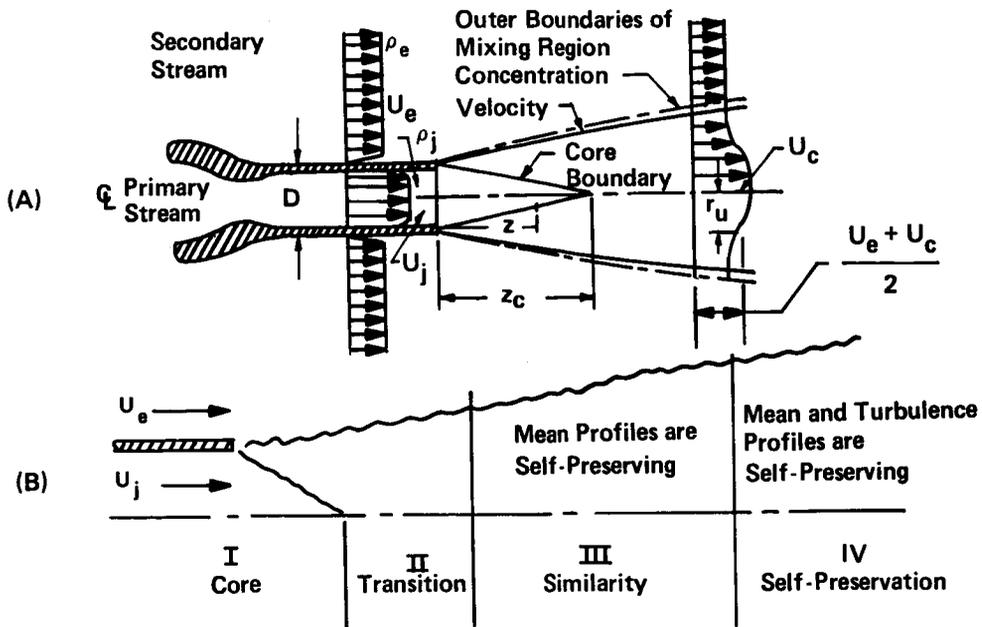
Figure 1.- Schematic of coaxial turbulent jet and definition of mixing regions.
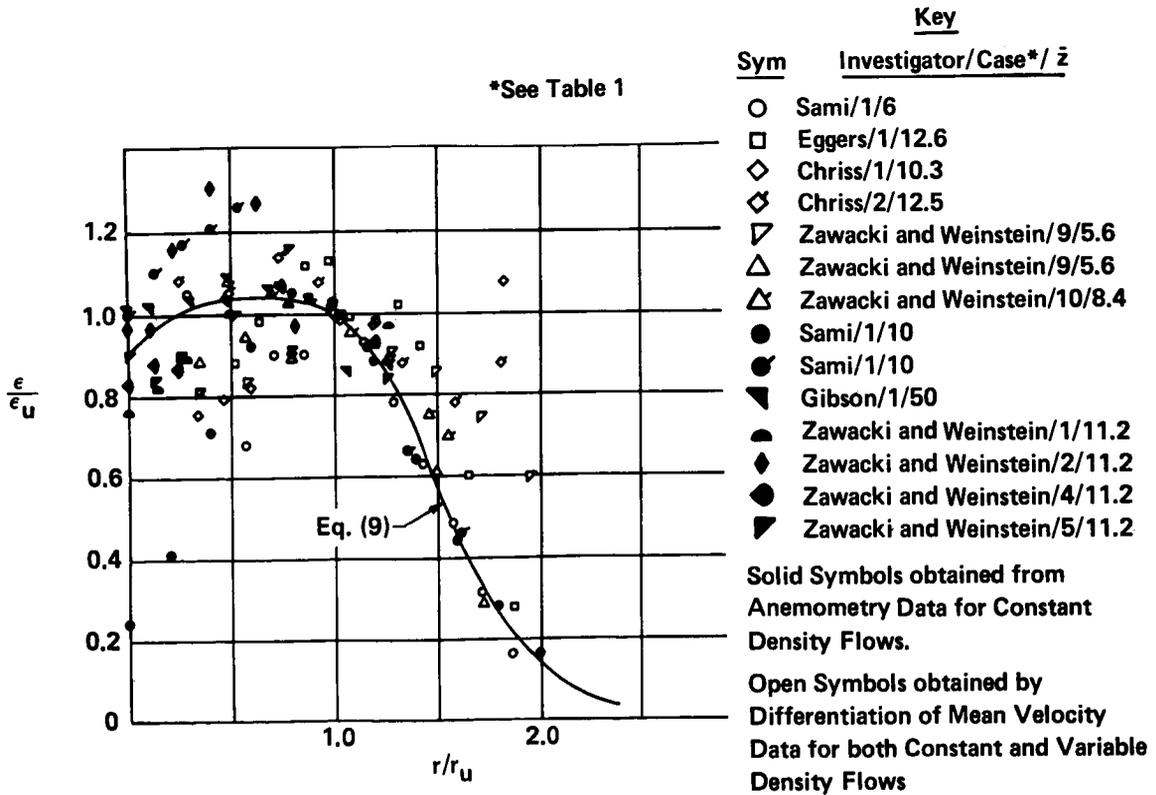
Figure 2.- Radial variation of ϵ/ϵ_u.
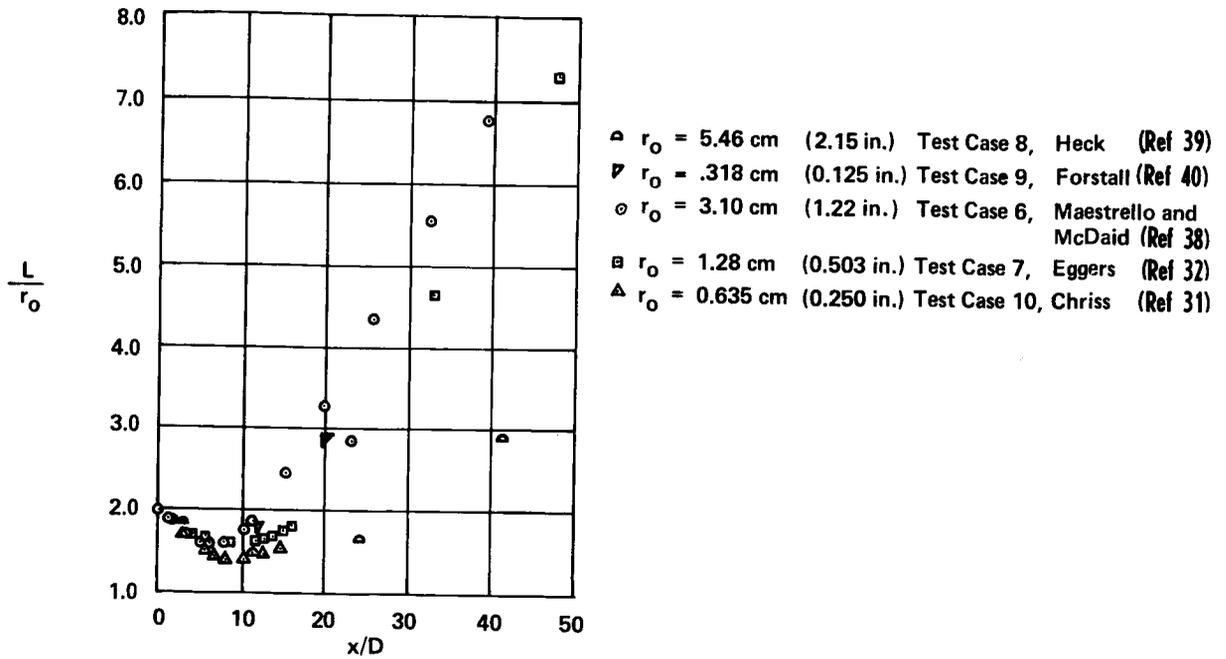
Figure 3.- Predicted characteristic length (eq. (7)).

Legend for Figure 3:

△ r_o = 5.46 cm (2.15 in.) Test Case 8, Heck (Ref 39)
▽ r_o = .318 cm (0.125 in.) Test Case 9, Forstall (Ref 40)
⊙ r_o = 3.10 cm (1.22 in.) Test Case 6, Maestrello and McDaid (Ref 38)
⊟ r_o = 1.28 cm (0.503 in.) Test Case 7, Eggers (Ref 32)
△ r_o = 0.635 cm (0.250 in.) Test Case 10, Chriss (Ref 31)

⊙ Exp., Maestrello and McDaid (Ref 38)
— Predicted

u_o = 211.2 m/sec (693 ft/sec)

r_o = 3.10 cm (1.22 in.)
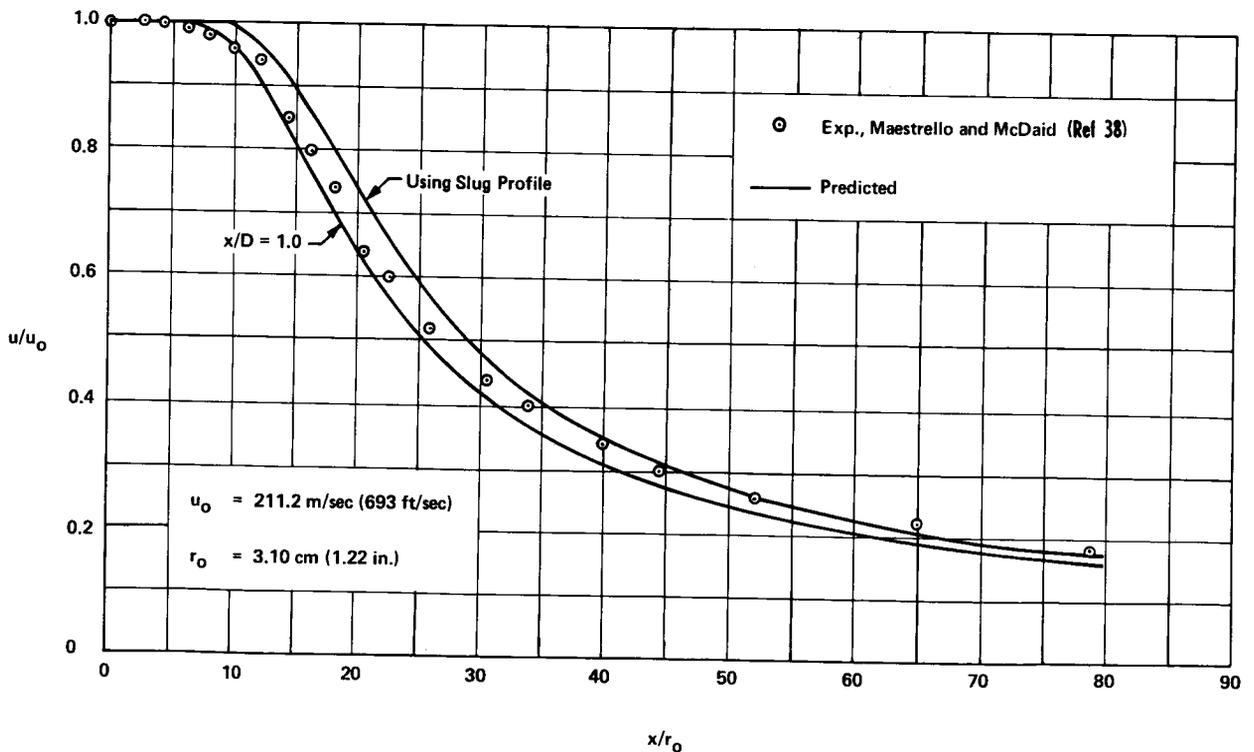
Figure 4.- Predicted and experimental center-line velocity for test case 6 (Maestrello and McDaid (ref. 38)).
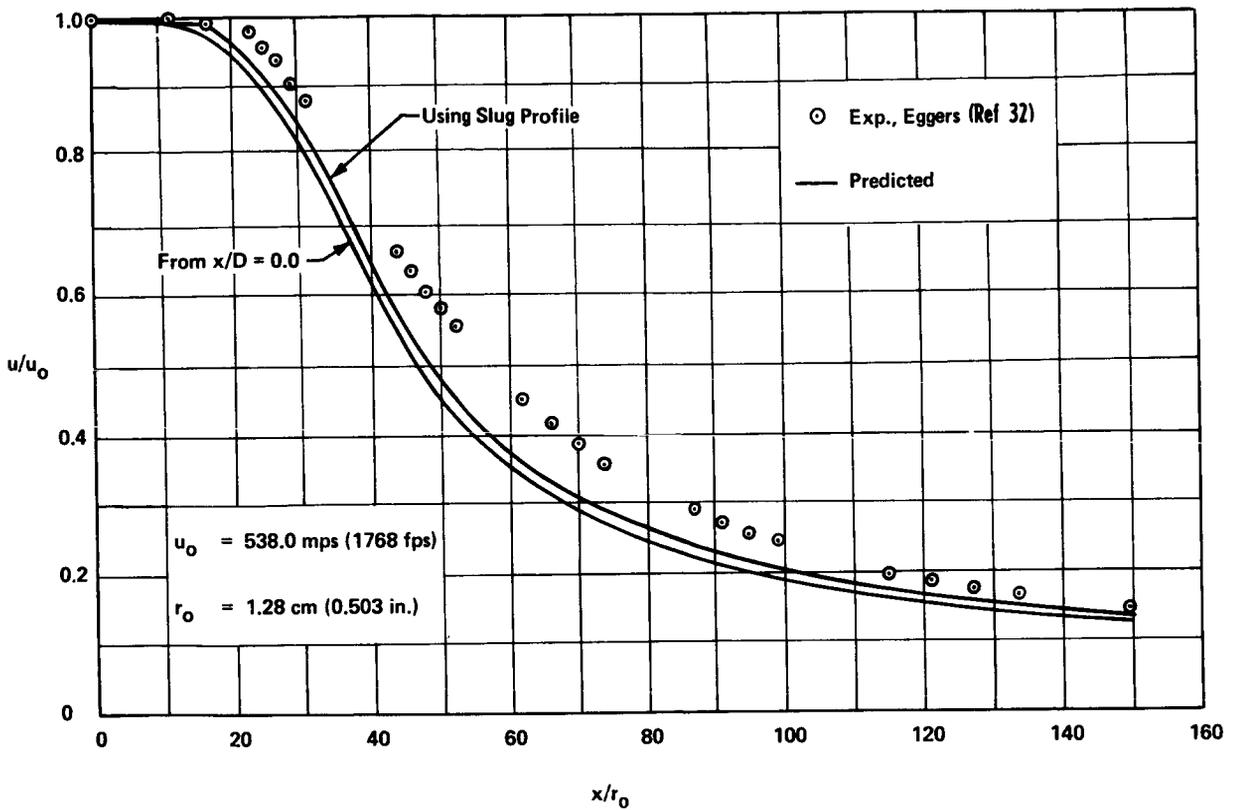
(a) Center-line velocity.

Figure 5.- Comparison of predicted and experimental velocities for test case 7 (Eggers (ref. 32)).
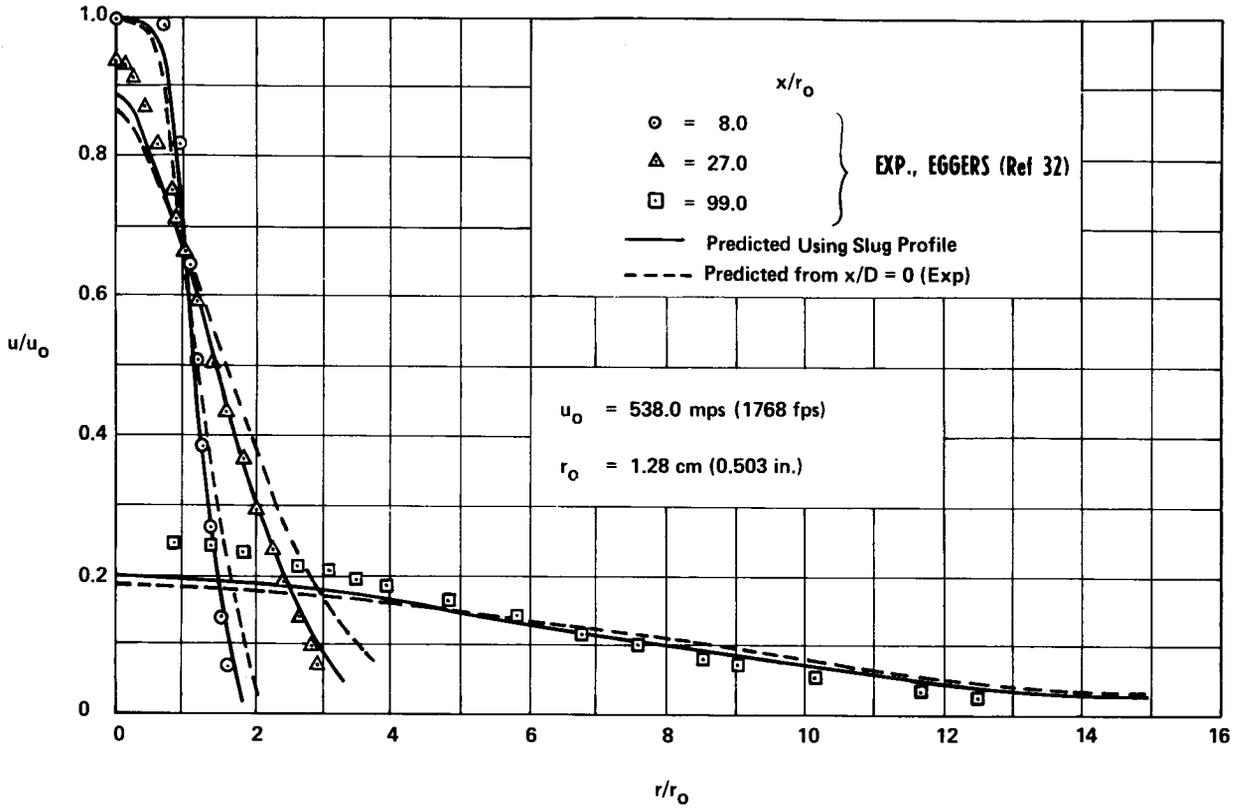
(b) Axial velocity against distance from center line.

Figure 5.- Concluded.
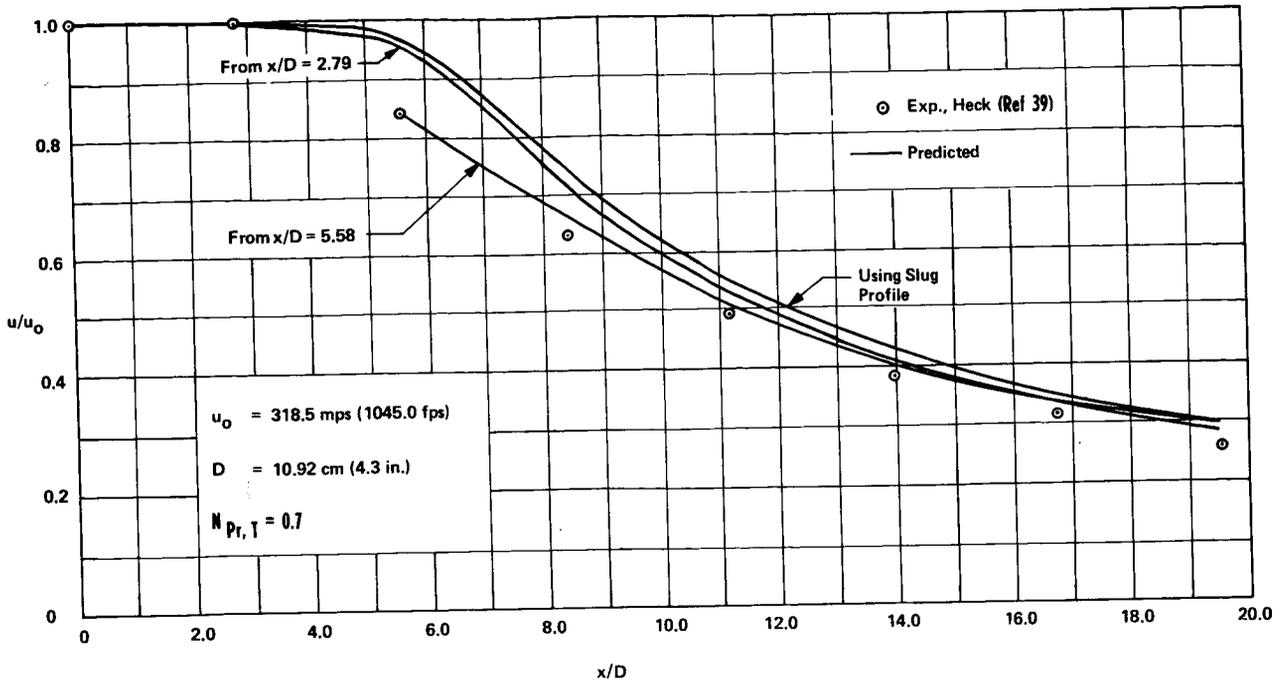
(a) Center-line velocity.
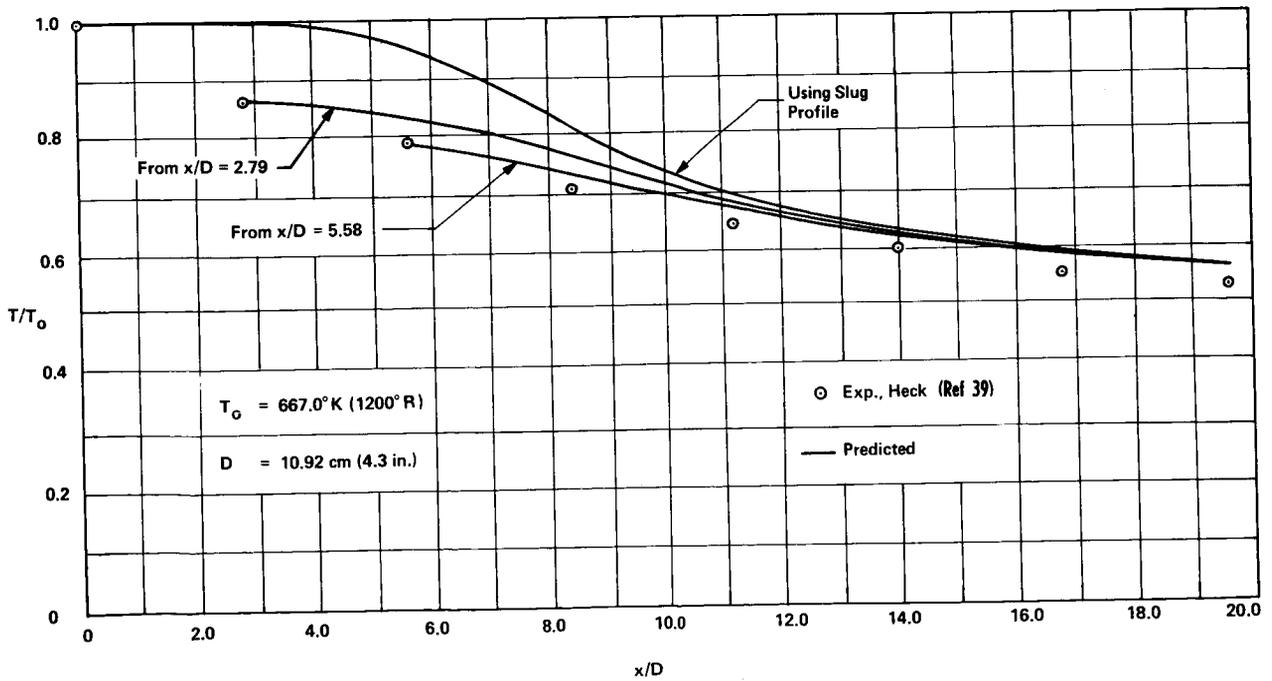
(b) Center-line total temperature.

Figure 6.- Comparison of predicted and experimental velocities and total temperatures for test case 8 (Heck (ref. 39)).
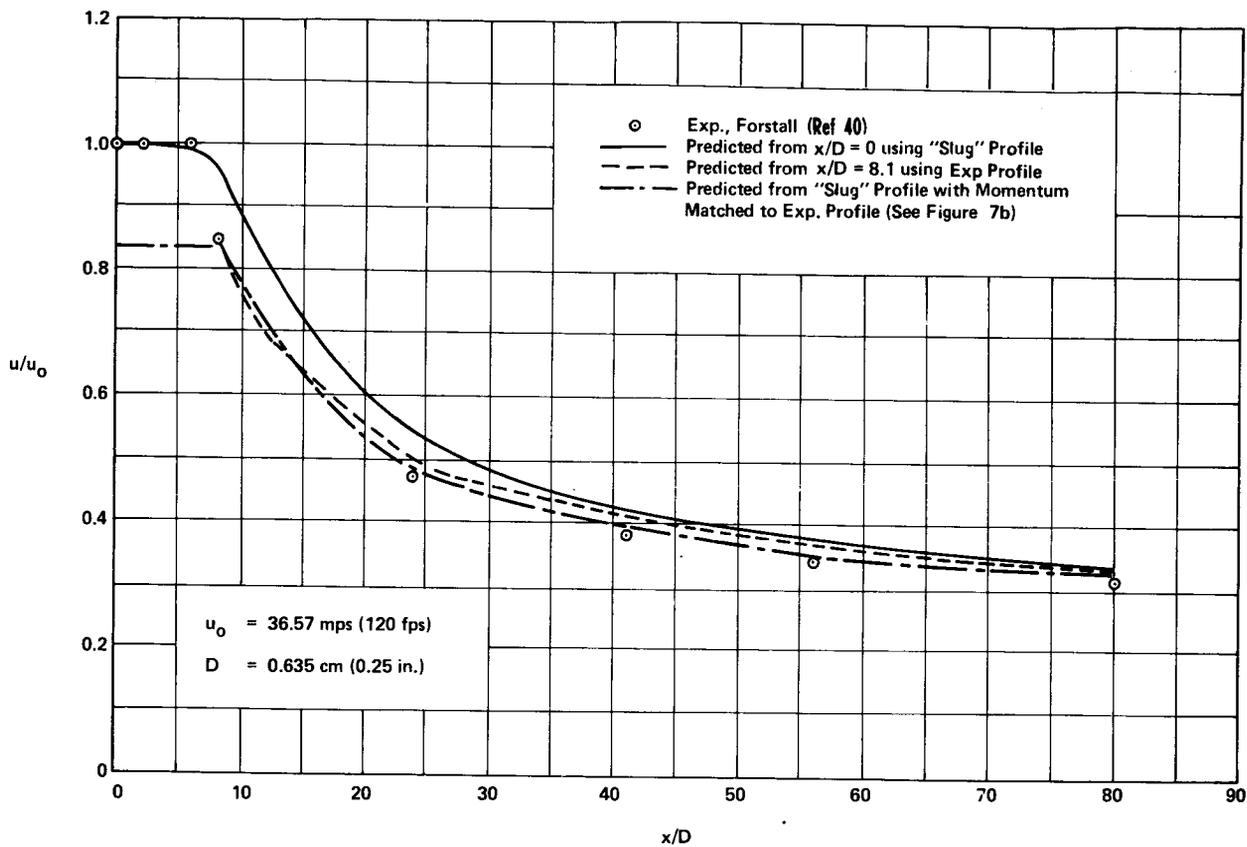
(a) Predicted and experimental center-line velocity

Figure 7.- Velocity and slug profiles for test case 9 (Forstall (ref. 40)).
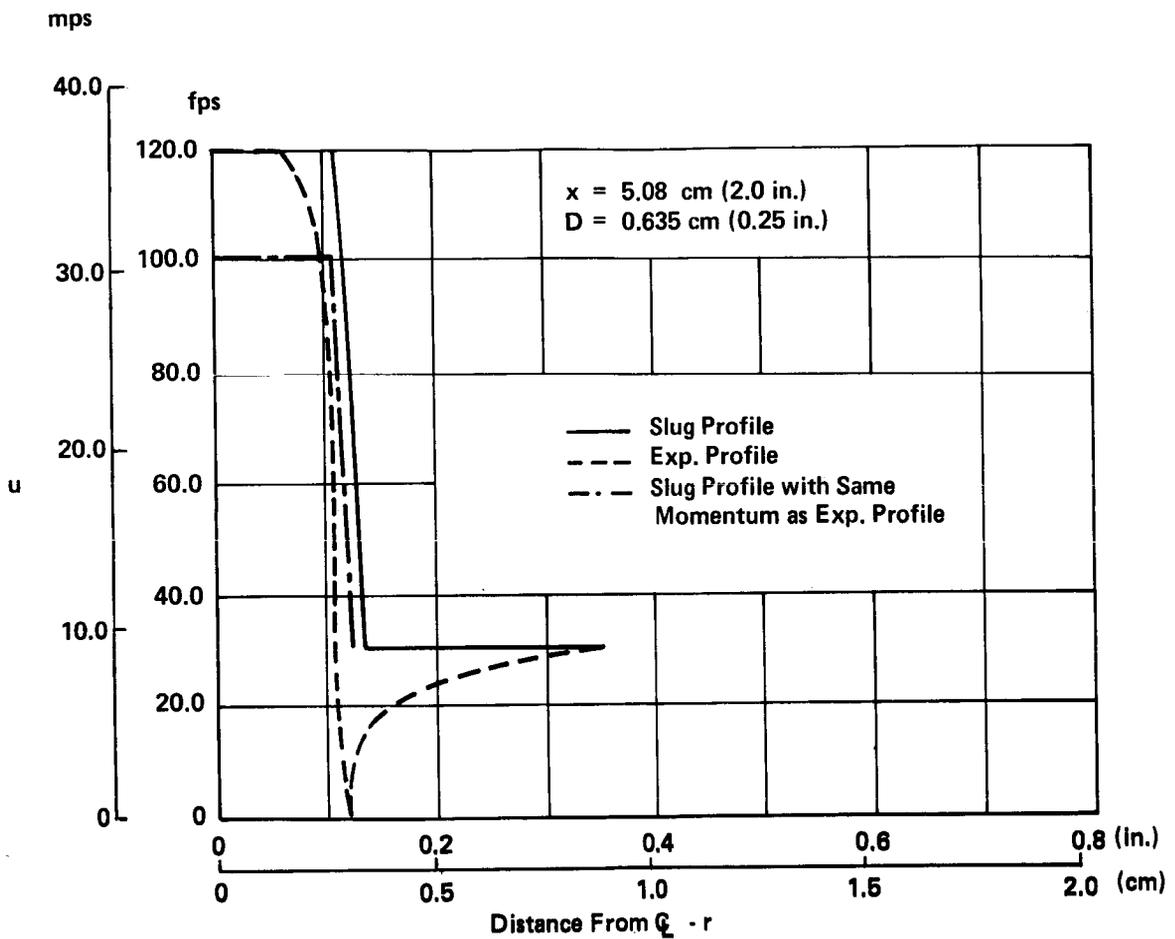
(b) Experimental and assumed slug profile at x/D = 0.

Figure 7.- Concluded.
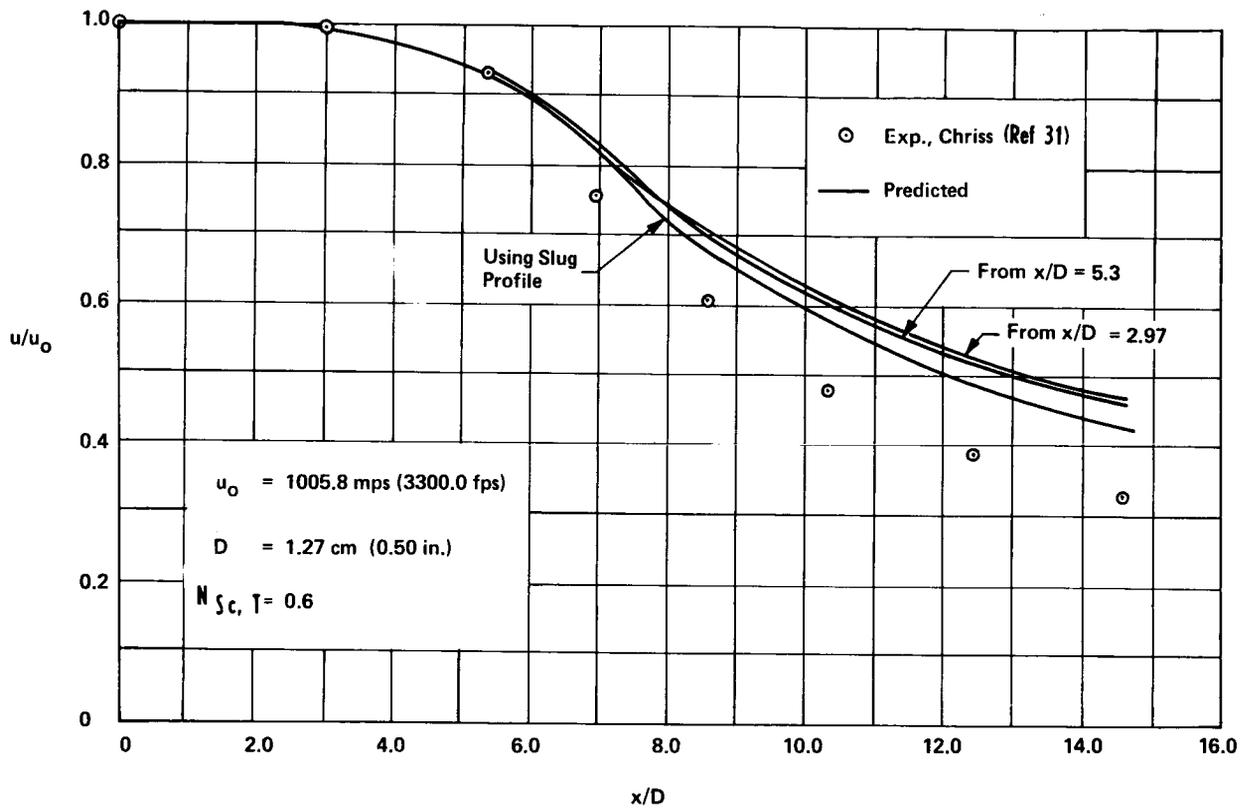
(a) Predicted and experimental center-line velocity.

Figure 8.- Velocities and H_2 mass fraction for test case 10 (Chriss (ref. 31)).
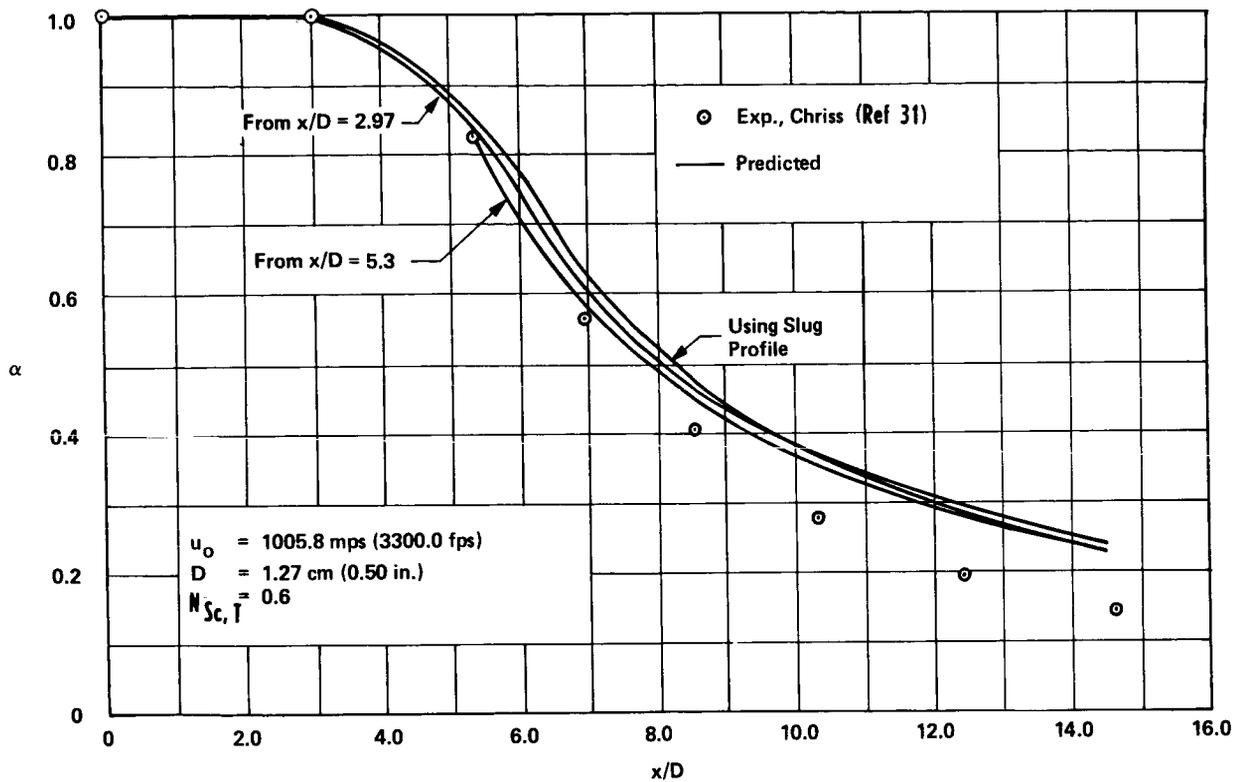
(b) Predicted and experimental center-line H_2 mass fraction.

Figure 8.- Continued.
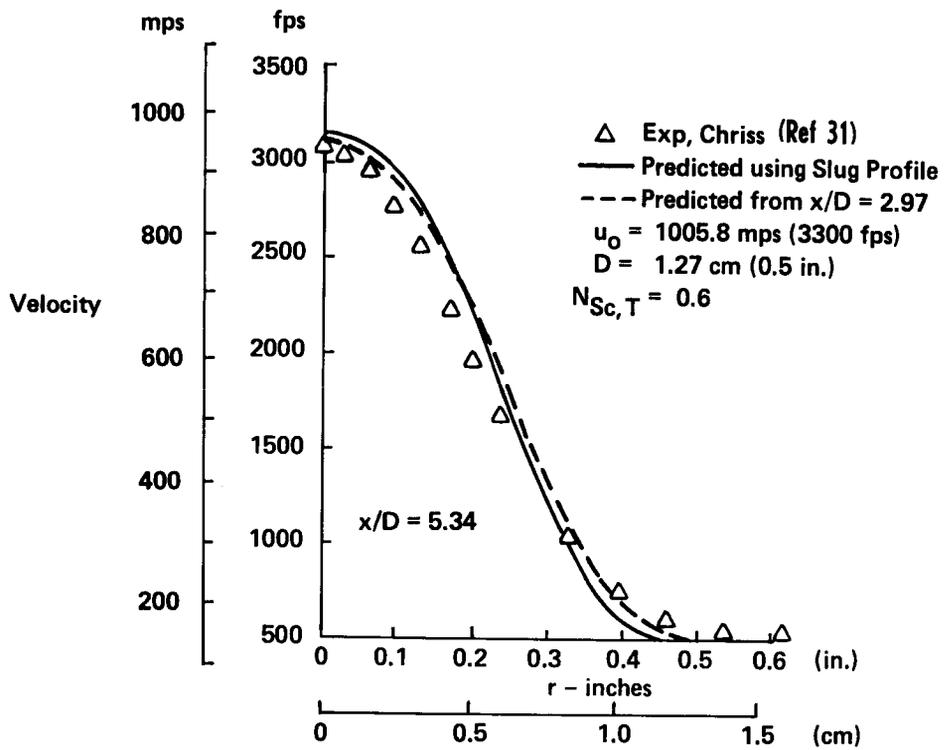
(c) Predicted and experimental axial velocity as a function of distance from center line at x/D = 5.34.

Figure 8.- Concluded.
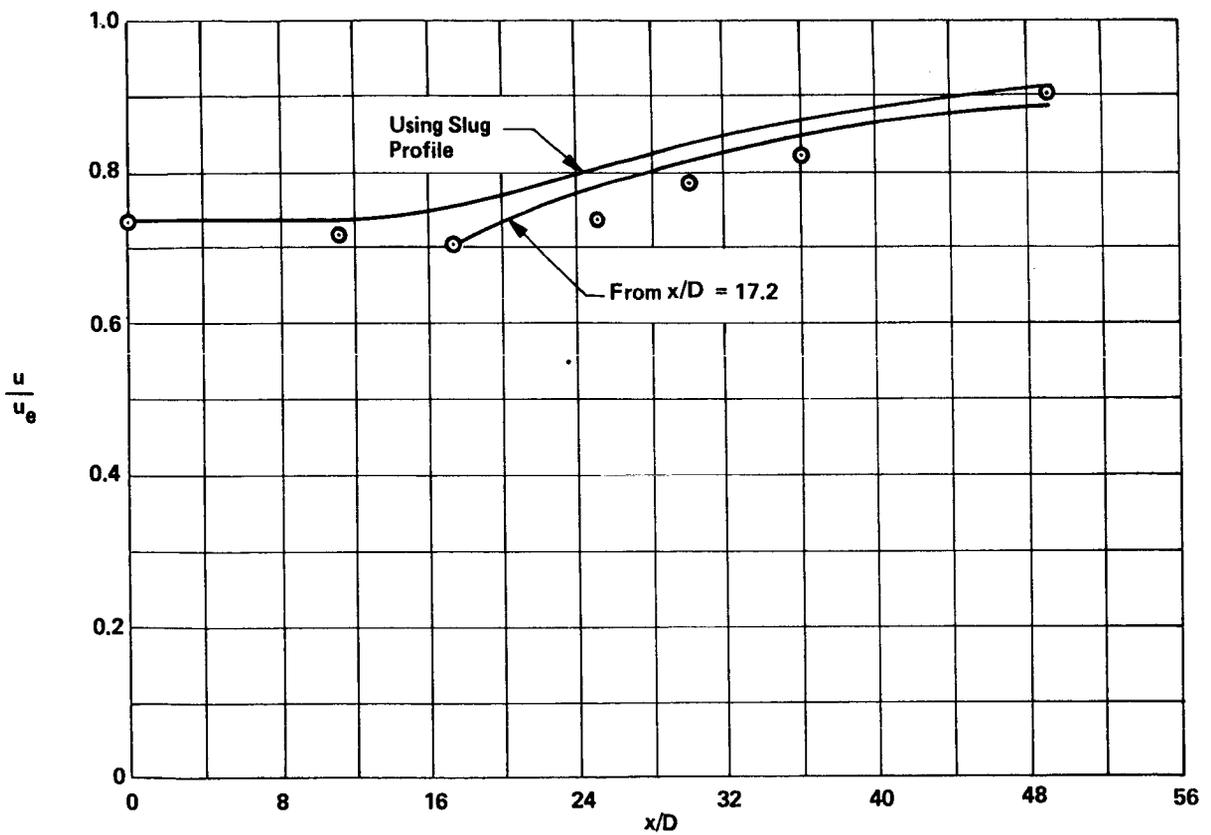
Figure 9.- Predicted and experimental center-line velocity for test case 11 (Eggers and Torrence (ref. 7)).

u_o = 1074.1 mps (3524.0 fps)   ⊙ Exp., Eggers (Ref 41)

D = 1.16 cm (0.456 in.)   —— Predicted

Using Slug Profile

From x/D = 9.6

u/u_o

x/D

(a) Predicted and experimental center-line velocity.

Figure 10.- Velocities and H_2 mass fraction for test case 12 (Eggers (ref. 41)).

D = 1.16 cm (0.456 in.)

$N_{Sc,T}$ = 0.9

⊙ Exp., Eggers (Ref 41)

── Predicted

Using Slug Profile

From x/D = 9.6
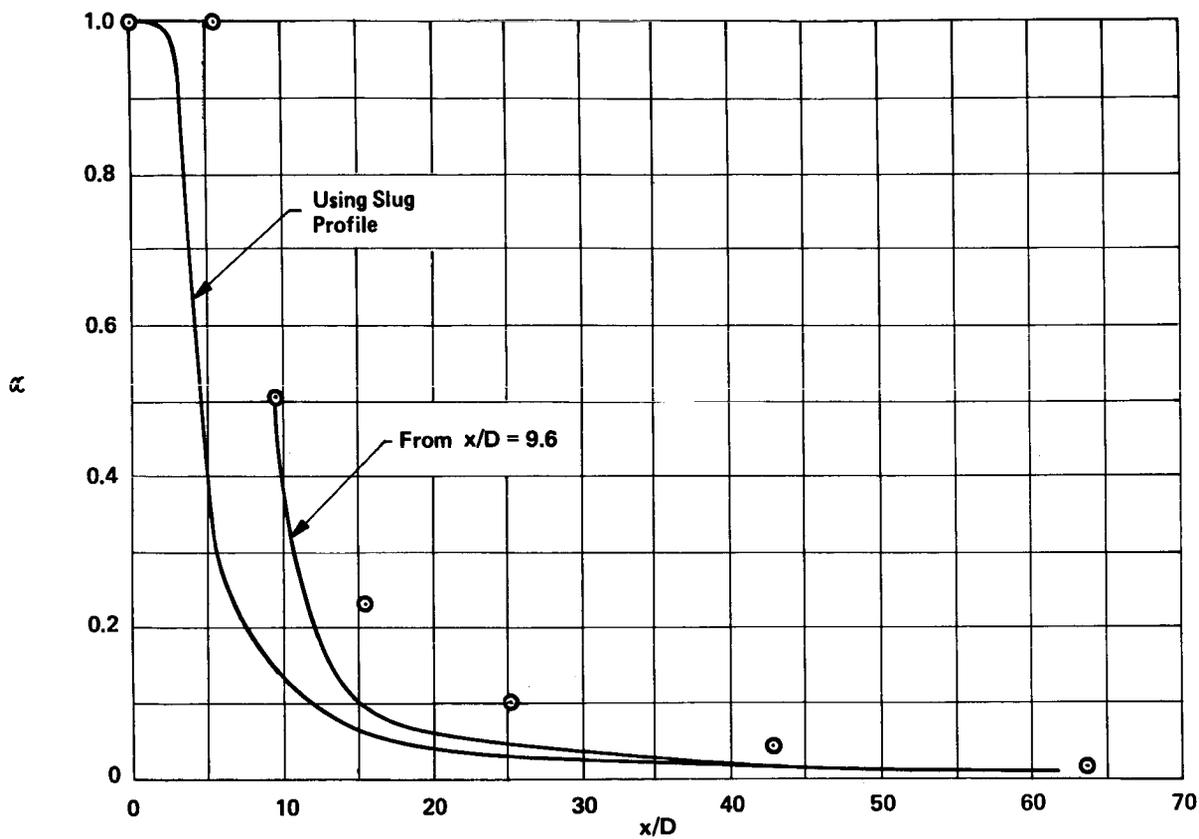
(b) Predicted and experimental center-line H_2 mass fraction.

Figure 10.- Concluded.
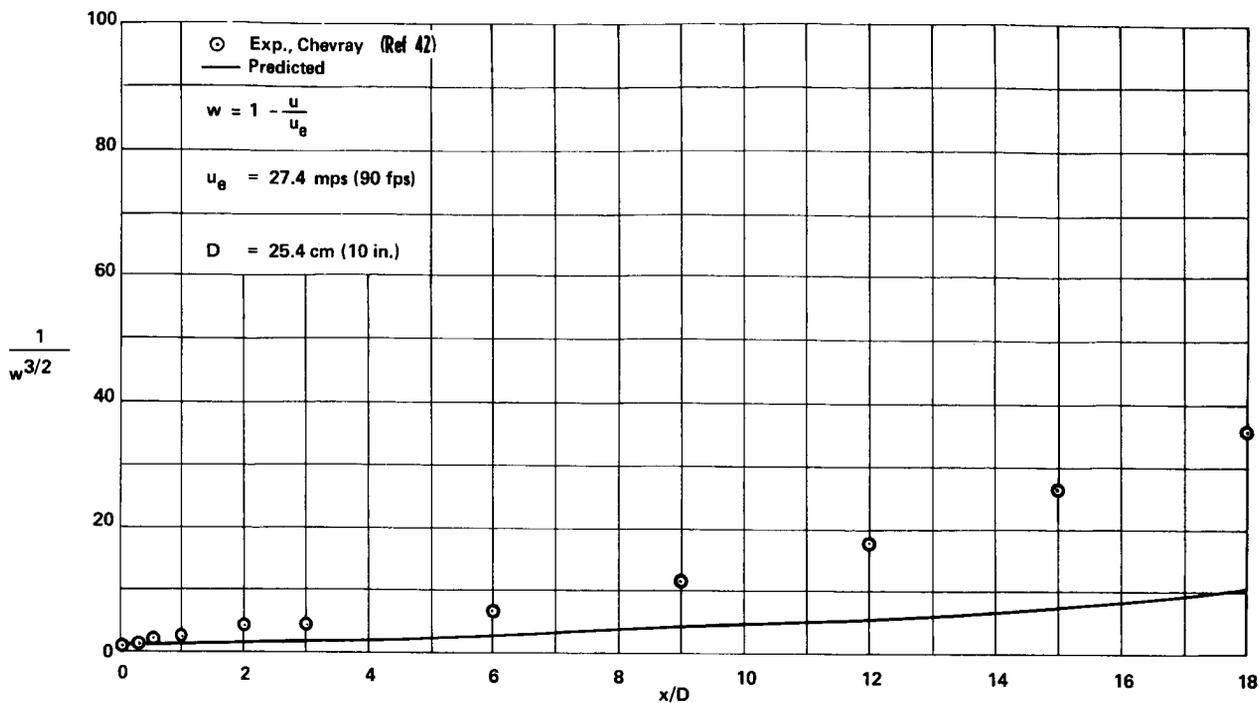
(a) Predicted and experimental center-line velocity. $(1 - u/u_e)^{-3/2}$ as a function of x/D.
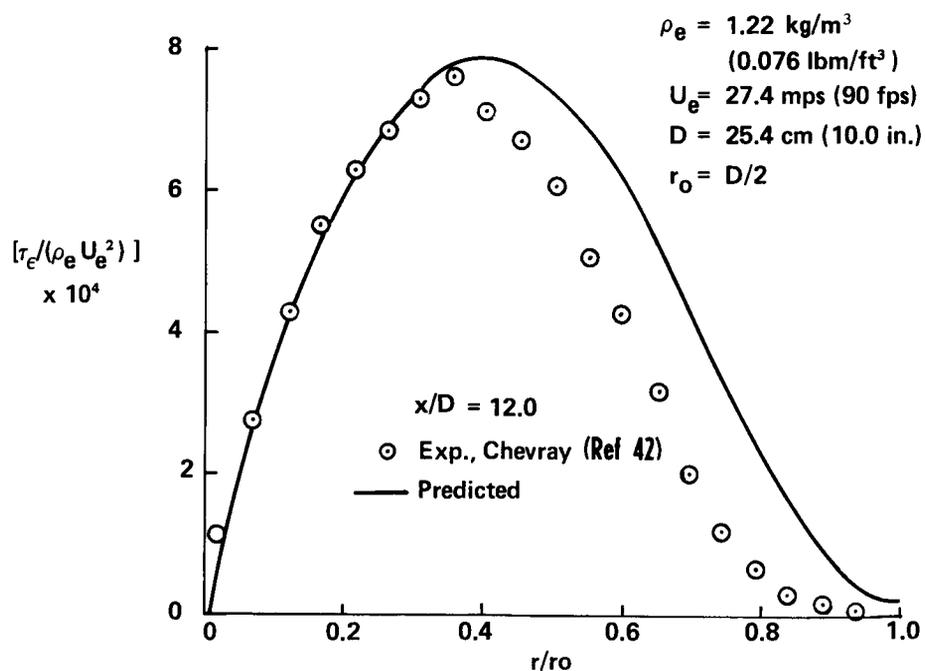
(b) Predicted and experimental shear stress profile at x/D = 12.0.

Figure 11.- Velocities and shear stress profiles for test case 15 (Chevray (ref. 42)).

$$w = 1 - \frac{u}{u_e}$$

u_e = 618.1 mps (2029 fps)

D = 0.396 cm (0.156 in.)

⊙　Exp., Demetriades (Ref 43)

——　Predicted
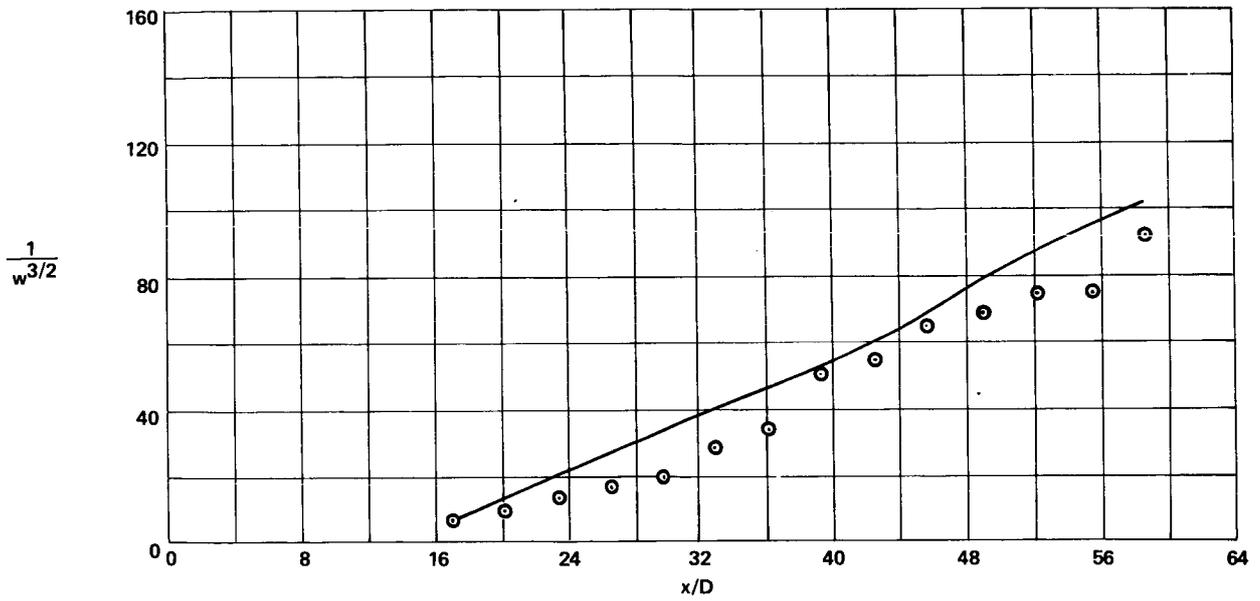
Figure 12.- Predicted and experimental center-line velocity for test case 17 (Demetriades (ref. 43)).
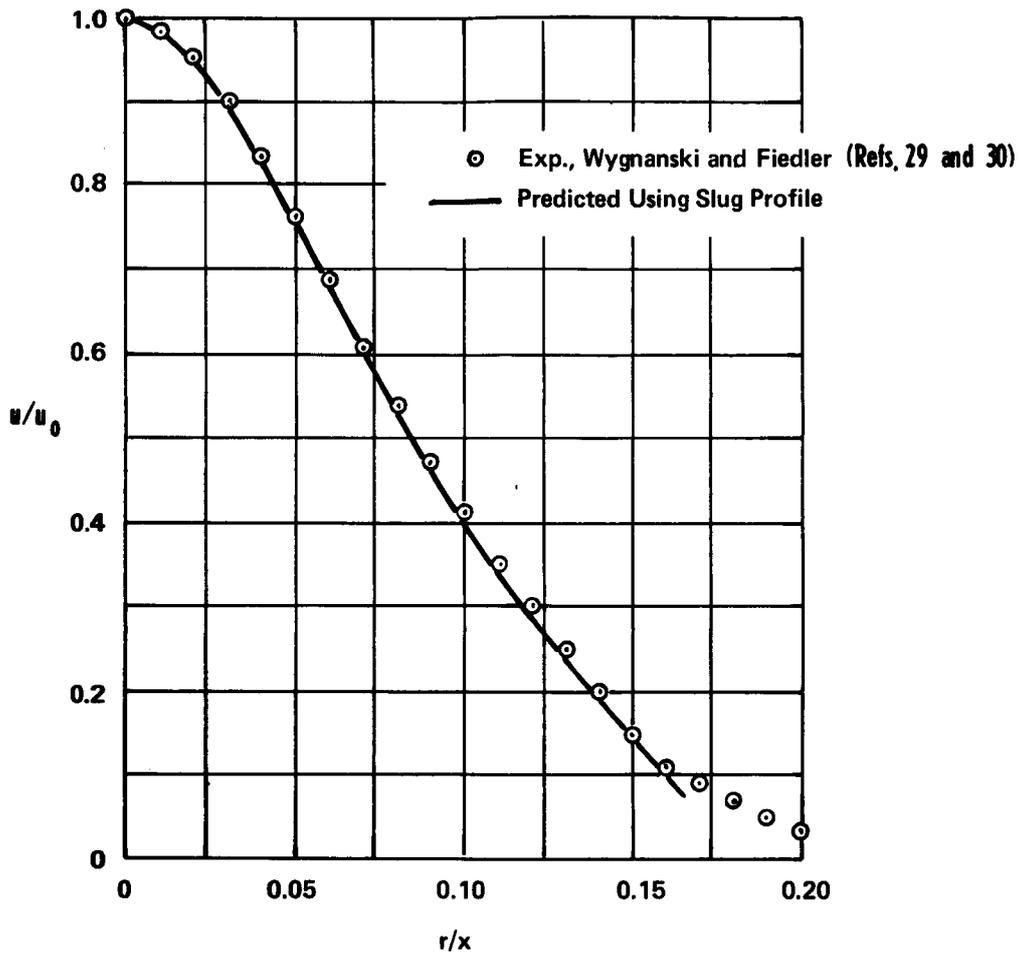
Figure 13.- Velocity profile in similarity coordinates for test case 18 (Wygnanski and Fiedler (refs. 29 and 30)).
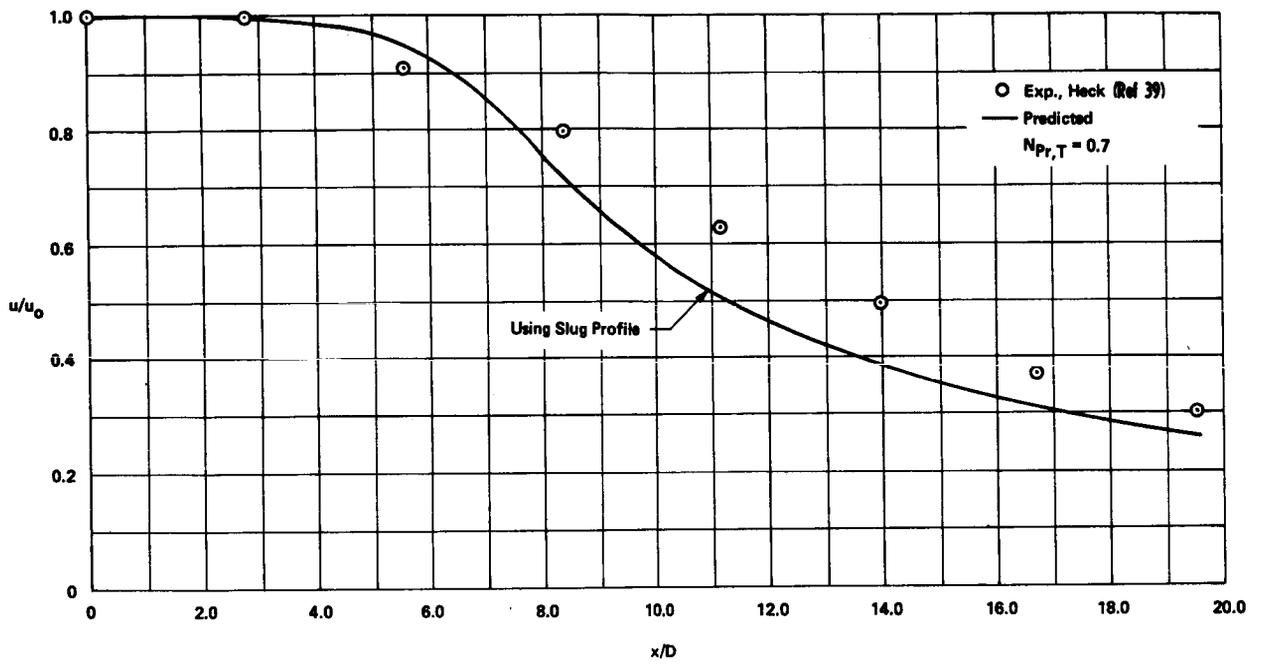
Figure 14.- Predicted and experimental center-line velocity for test case 19 (Heck (ref. 39)).
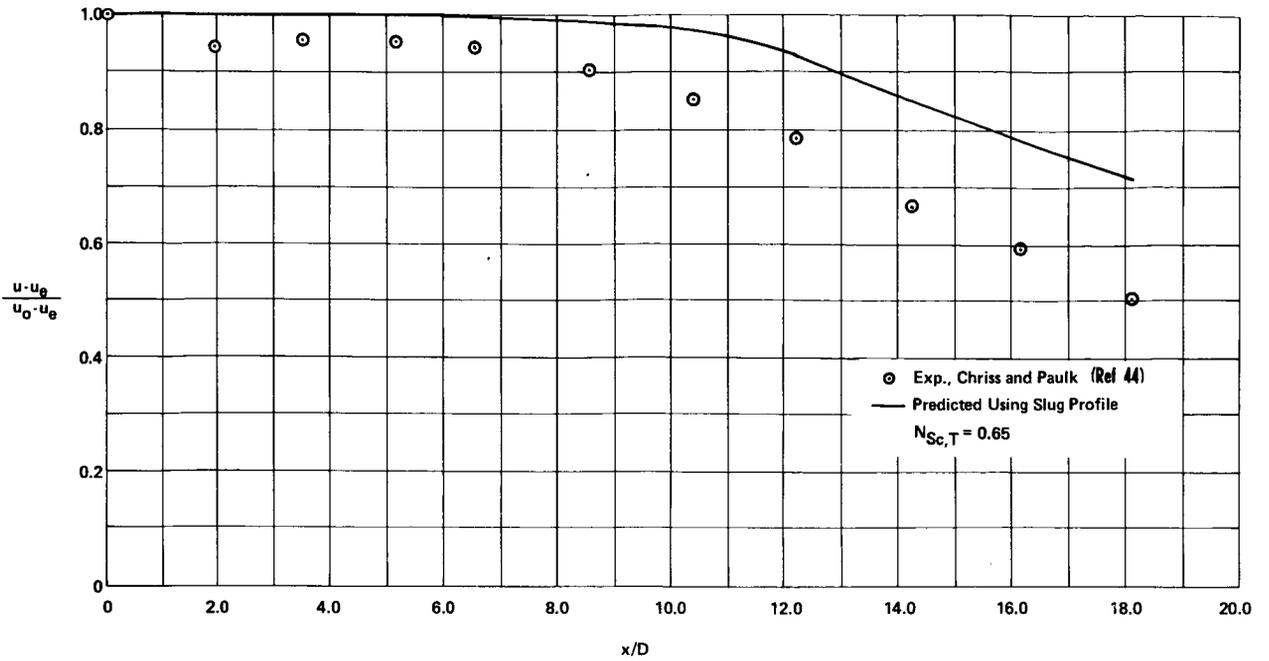
(a) Predicted and experimental center-line velocity.
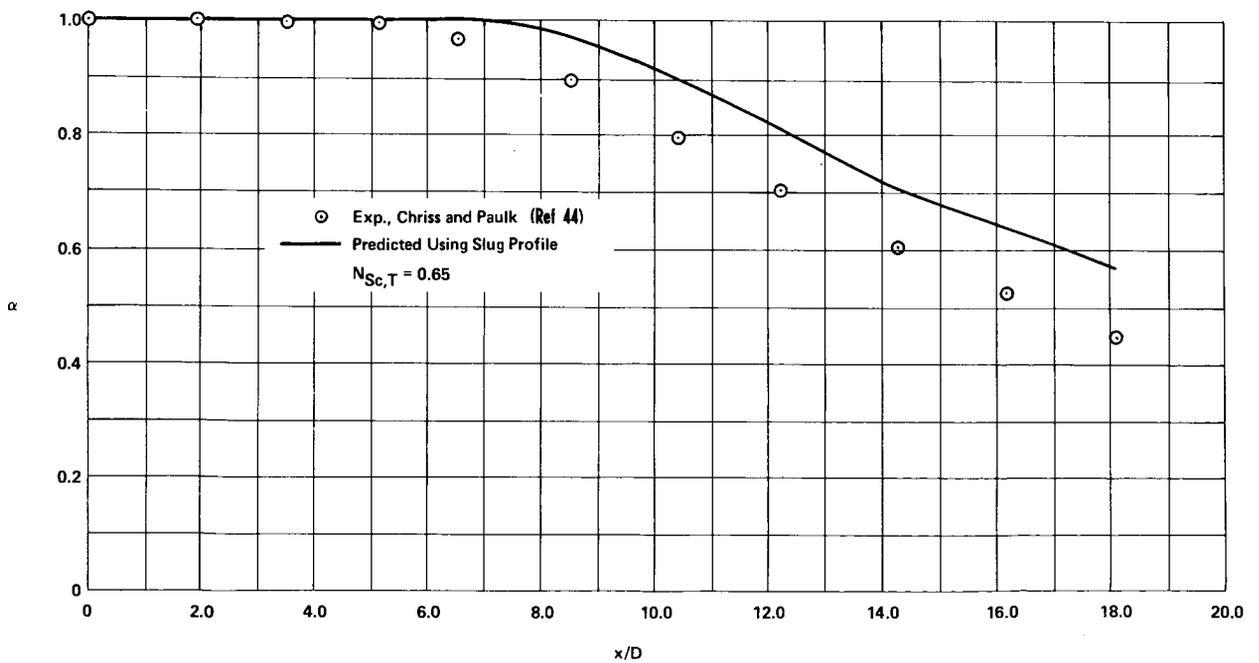
(b) Predicted and experimental center-line H_2 mass fraction.

Figure 15.- Velocities and mass fraction for test case 20 (Chriss and Paulk (ref. 44)).
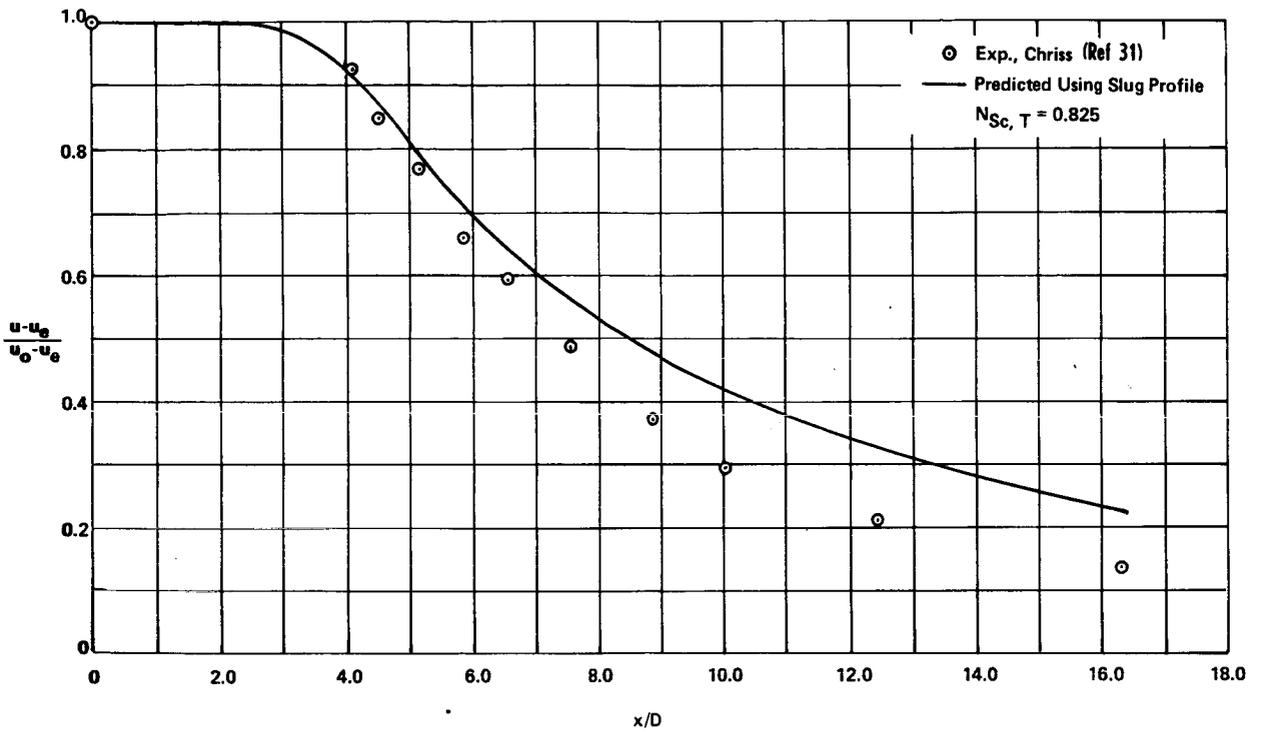
(a) Predicted and experimental center-line velocity.

Figure 16.- Velocities and mass fraction for test case 21 (Chriss (ref. 31)).
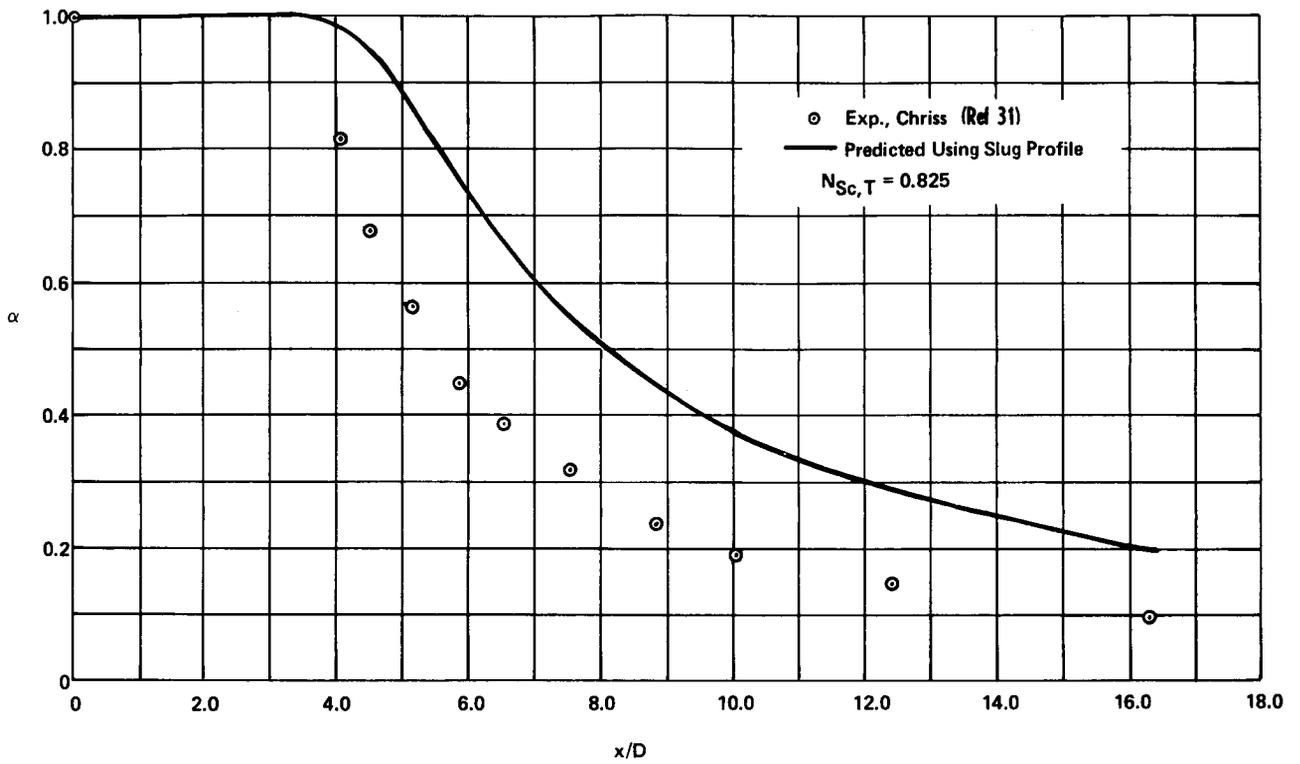
(b) Predicted and experimental center-line H_2 mass fraction.

Figure 16.- Concluded.
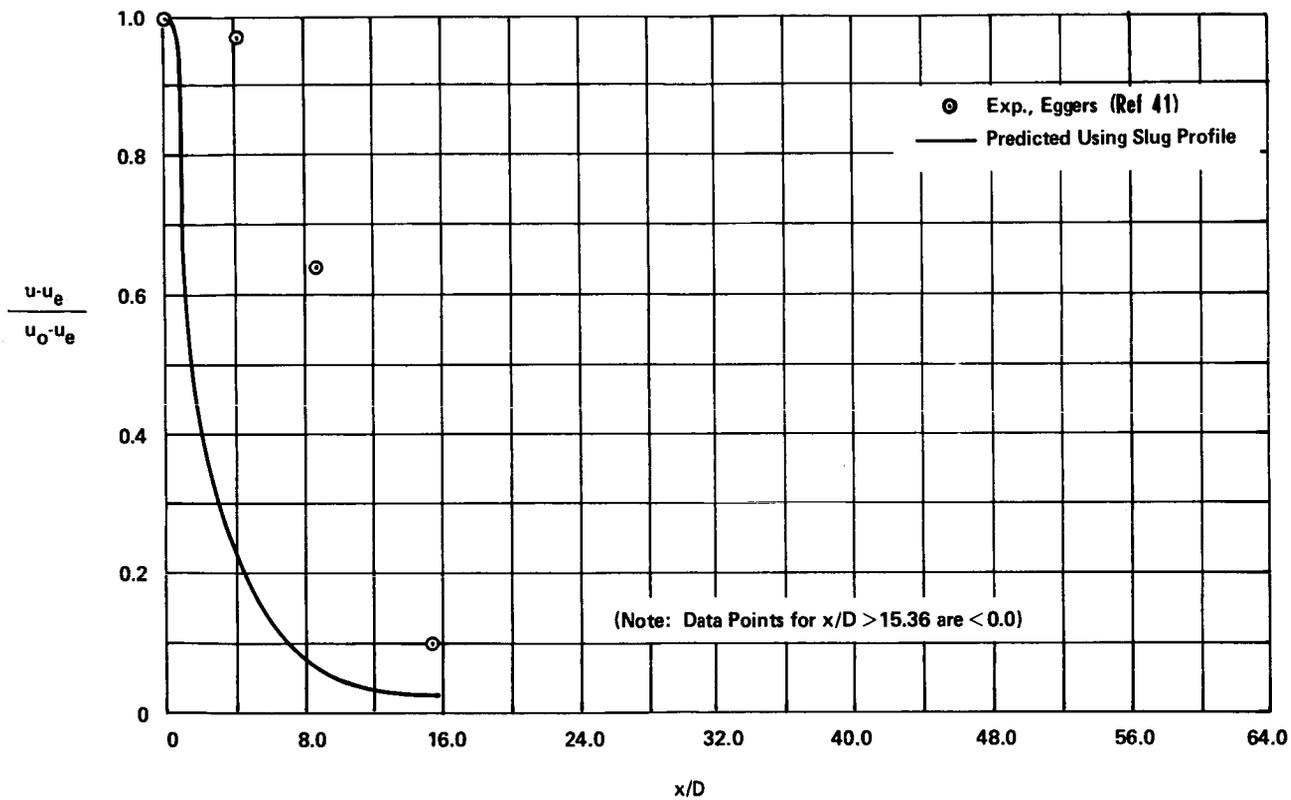
Figure 17.- Predicted and experimental center-line velocity for test case 22 (Eggers (ref. 41)).
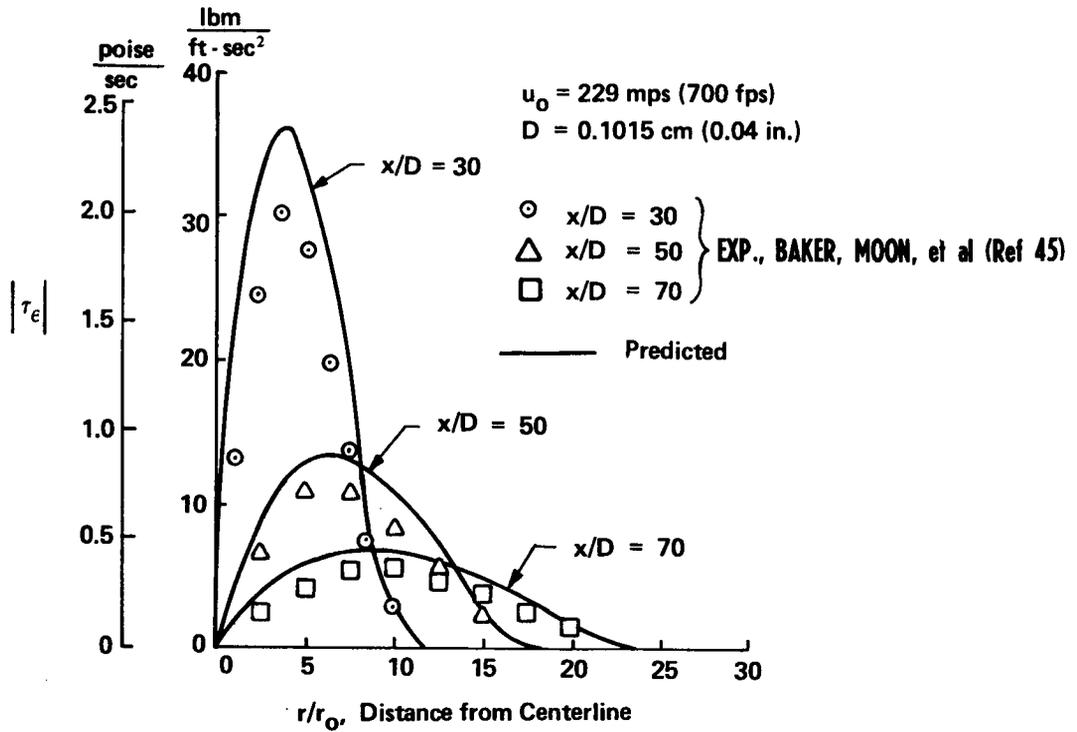
Figure 18.- Shear stress profiles at x/D = 30, 50, and 70 for data of Baker, Moon, et al. (ref. 45).
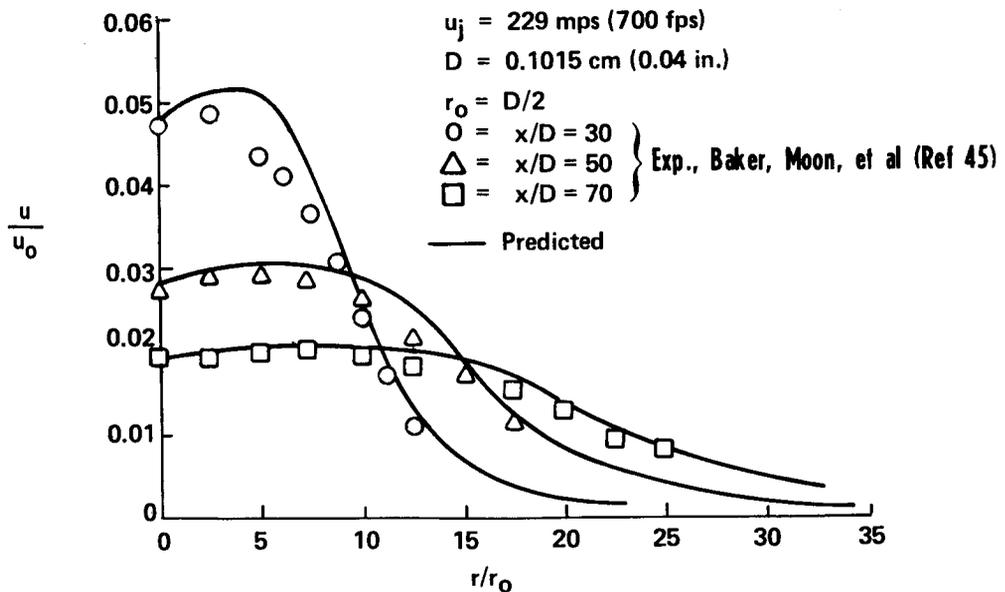
Figure 19.- Predicted and experimental axial turbulent intensity profiles at x/D = 30, 50, and 70.
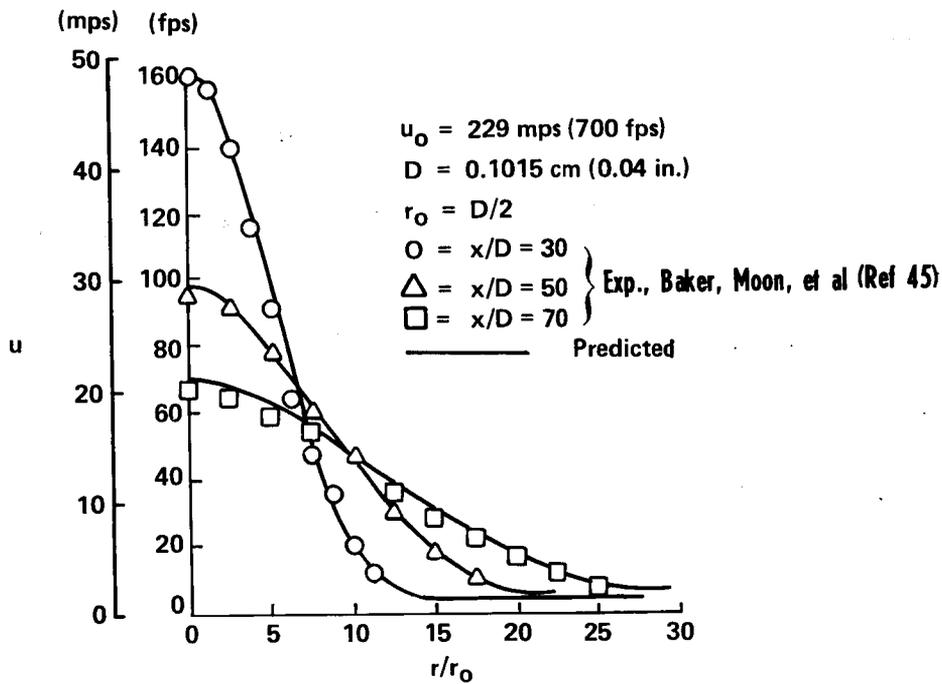
Figure 20.- Predicted and experimental axial velocity profiles at x/D = 30, 50, and 70.
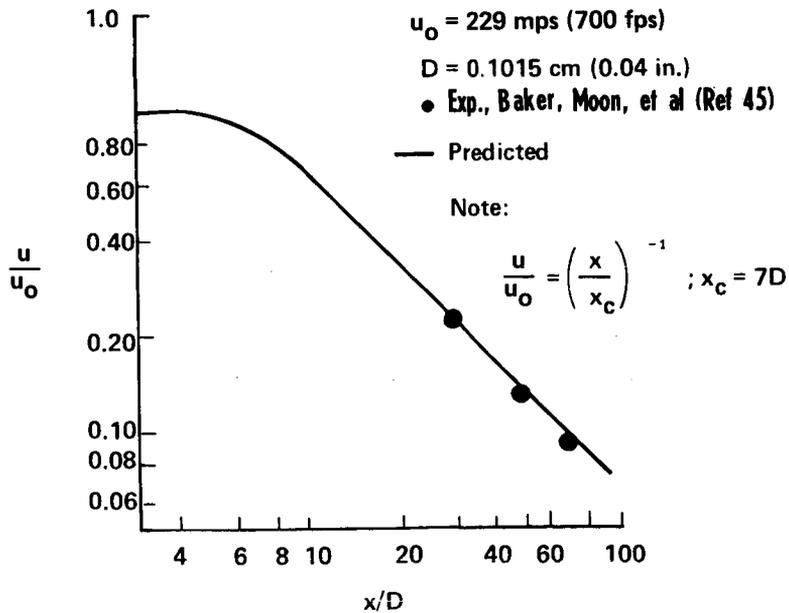
Figure 21.- Predicted and experimental center-line velocity.

DISCUSSION

S. Corrsin: This is a trivial remark, but on the figure showing eddy viscosity ϵ versus radial distance r you have a finite slope of ϵ at the center line of the axis of the jet. I wonder whether it would be better to have a horizontal slope there.

J. H. Morgenthaler: Of course, the center line is an axis of symmetry; however, because $(\partial u/\partial r)_{\text{C}} = 0$, it is not possible (or necessary) to define $(\partial \epsilon/\partial r)_{\text{C}}$.

I. E. Alber: Also, with respect to your eddy viscosity model, I noticed that you had the eddy viscosity ϵ proportional to u'^2. Nominally, from dimensional analysis, one would take ϵ proportional to u'. Is there any reason that you chose that over the more conventional scheme?

J. H. Morgenthaler: Steve, would you like to answer that one?

S. W. Zelazny: The proportionality you are referring to (eq. (5)) was obtained by assuming (1) the shear stress is directly proportional to the turbulence kinetic energy, an assumption used in a number of the Workshop papers using the turbulence kinetic energy approach, (2) the ratio of the transverse turbulence intensity to the axial turbulence intensity is independent of radial position, and (3) the shear correlation coefficient is directly proportional to the partial derivative of the axial velocity with respect to the radial coordinate, that is, $\partial U/\partial r$. The relation, ϵ proportional to u'^2, also may be obtained from dimensional analysis if it is assumed that the eddy viscosity is functionally dependent on density u'^2 and the maximum value of $\partial U/\partial r$ at a given axial station.

J. H. Morgenthaler: In other words, we did not pull the relation out of our hat.

M. V. Morkovin: Concerning the same point, how do you use equation (5)? Do you use ϵ just to evaluate u'^2? It is not used in the development of other relationships, is it?

S. W. Zelazny: Equation (5) was used to develop the empirical expression, $G(r/r_u)$ of equation (9) describing the radial variation of eddy viscosity and turbulence intensity. It showed that both eddy viscosity "data" and turbulence intensity data could be used to obtain an approximation for ϵ/ϵ_u and $(\rho u'^2)/(\rho u'^2)_u$ consistent with the assumptions listed in my reply to Dr. Alber. It is not true that ϵ is just used to evaluate u'^2 since ϵ is essential for prediction of the mean values.

J. H. Morgenthaler: In figure 2 of the paper, there are open symbols and closed symbols which didn't show up very well on the slide, but as you can see, some points were obtained by direct differentiation of the mean data, and some were obtained directly from hot-wire turbulence measurements.

M. V. Morkovin: But I'm saying, that all you are trying to do is to fit some transverse variation of ϵ. In your computations as you are marching in the axial direction, the effect of transverse variation does not influence predictions since the function $G(r/r_u)$ is independent of z. That is, the transverse variation only affects prediction of the turbulence quantities, doesn't it?

J. H. Morgenthaler: The transverse variation of ϵ has a great influence on predictions, as is illustrated in the figure. The local value of ϵ greatly influences the rate of momentum transport as minor perturbations in ϵ have demonstrated during the development of the model. It is true, however, that the computation of mean quantities is not influenced by the prediction of turbulence intensity. In other words, the model may predict valid mean profiles but be considerably poorer in its predictions of turbulence quantities.

T. Cebeci: Well, let us have one more question before we take our coffee break.

S. C. Lee: I am looking at your figure 2 right now. I have a question related to this figure. It looks from the figure that the function $G(r/r_u)$ might be considered to be constant between $r/r_u = 0$ and $r/r_u = 1.5$. What effect would this assumption have on the predictions?

J. H. Morgenthaler: We believe the radial variation to be important based on our modeling experience. We have run a case which shows that the length of the transition region is significantly influenced as are mean quantities (see the figure). For example, the velocity at the $\mathcal{C}$ at $z = 50\,D$ (2.0 in.) was 92.0 ft/sec for $G(r/r_u)$ defined by equation (9), but was 64.3 ft/sec when the assumption was made that $G \equiv 1$.
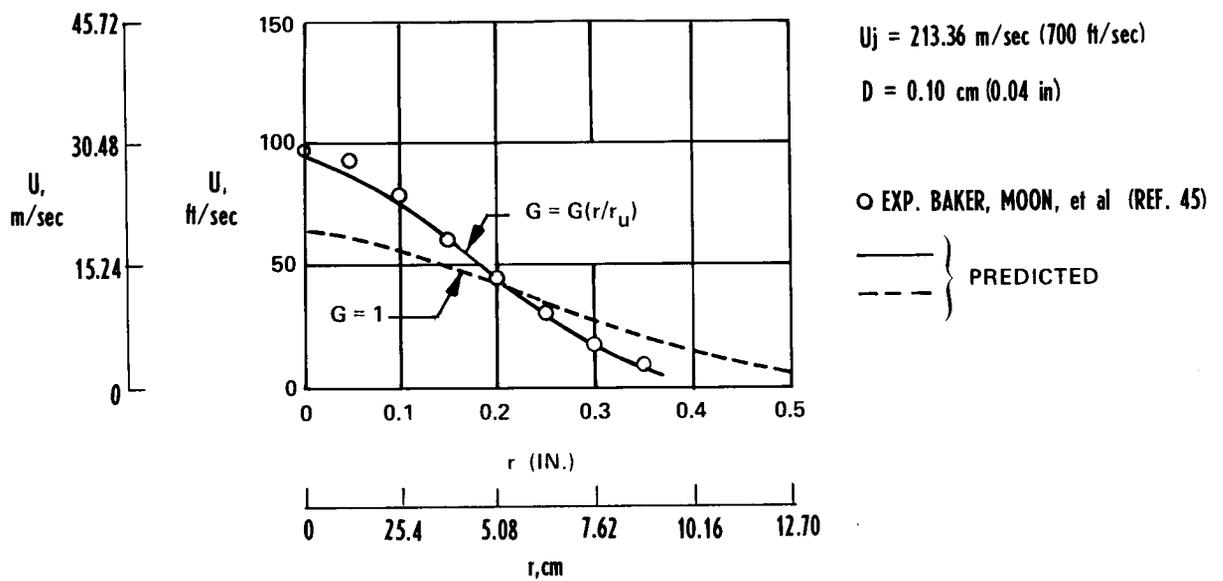
Figure 1.- Predicted velocity profiles at z/D = 50 showing effect of
including radial variation in eddy viscosity model.